Title

A Fickian Diffusion Model for the spreading of liquid plumes infiltrating in heterogeneous media

Journal

Trasnport in Porous Media, 24(1)

Author

Pruess, K.

Publication Date

1994-10-25

LBL-33914
UC-200, UC-250
Preprint

Lawrence Berkeley Laboratory
UNIVERSITY OF CALIFORNIA

EARTH SCIENCES DIVISION

Submitted to Water Resources Research

Dispersion of Immiscible Fluid Phases in Gravity-Driven Flow: A Fickian Diffusion Model

K. Pruess

June 1993

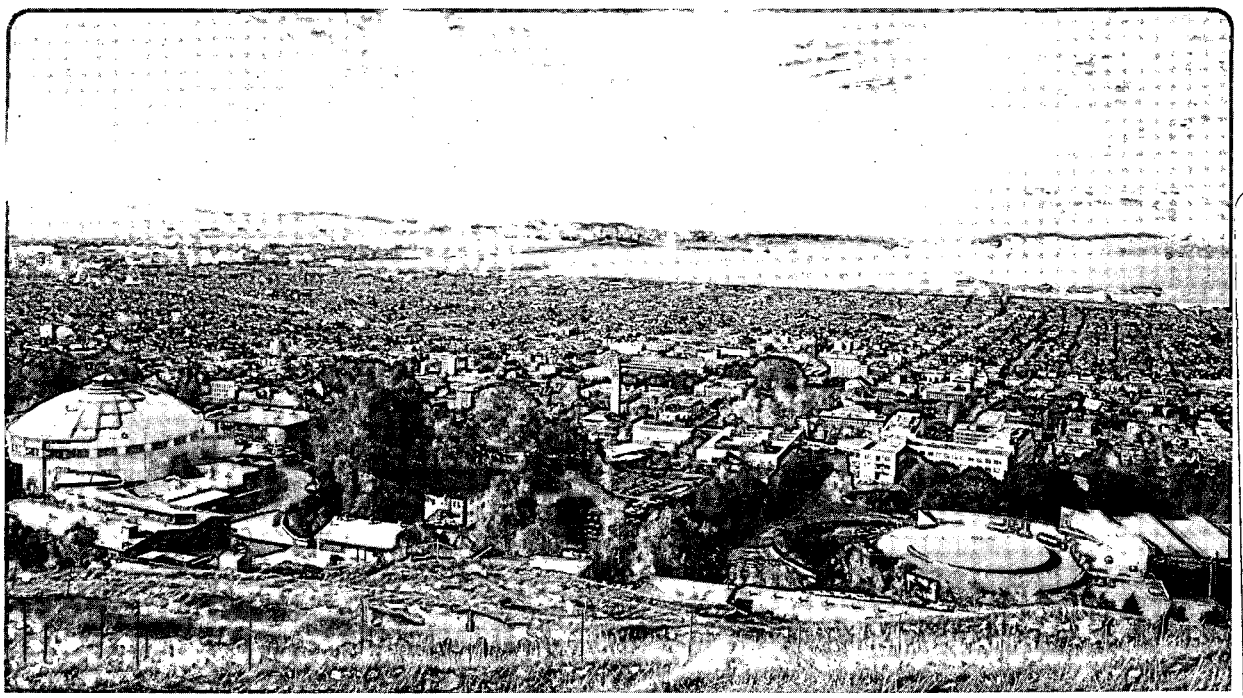

Prepared for the U.S. Department of Energy under Contract Number DE-AC03-76SF00098

DISCLAIMER

LBL-33914

Dispersion of Immiscible Fluid Phases in Gravity-Driven Flow: A Fickian Diffusion Model

Karsten Pruess

Earth Sciences Division
Lawrence Berkeley Laboratory
University of California
Berkeley, California 94720

June 1993

This work was supported in part by the Institut fuer Stroemungsmechanik, University of Hanover, Germany, and in part by the Assistant Secretary for Conservation and Renewable Energy, Geothermal Division, by the Assistant Secretary for Environmental Restoration and Waste Management, Office of Technology Development, and by the Director, Office of Civilian Radiactive Waste Management, Office of External Relations, administered by the Nevada Operations Office, U.S. Department of Energy, under U.S. Department of Energy Contract No. DE-AC03-76SF00098.

LBL-33914

DISPERSION OF IMMISCIBLE FLUID PHASES IN GRAVITY-DRIVEN FLOW: A FICKIAN DIFFUSION MODEL

Karsten Pruess

Earth Sciences Division, Lawrence Berkeley Laboratory

University of California, Berkeley, CA 94720

ABSTRACT

Infiltration of water and non-aqueous phase liquids (NAPLs) in the vadose zone gives rise to complex two- and three-phase immiscible displacement processes. Physical and numerical experiments have shown that ever-present small-scale heterogeneities will cause a lateral broadening of the descending liquid plumes. This behavior of liquid plumes infiltrating in the vadose zone is similar to the familiar transversal dispersion of solute plumes in single-phase flow. Noting this analogy we introduce a mathematical model for "phase dispersion" in multiphase flow as a Fickian diffusion process.

It is shown that the driving force for phase dispersion is the gradient of relative permeability, and that addition of a phase-dispersive term to the governing equations for multiphase flow is equivalent to an effective capillary pressure which is proportional to the logarithm of the relative permeability of the infiltrating liquid phase. Finite difference discretization of the phase-dispersive flux is discussed, and the relationship between "physical" phase dispersion and numerical dispersion arising from finite-difference discretization is established. Effects of phase dispersion are demonstrated by numerical simulation for three illustrative problems, including water and NAPL infiltration from a

localized source, and water injection into depleted vapor-dominated geothermal reservoirs. It is found that a small amount of phase dispersion can completely alter the behavior of an infiltrating NAPL plume, and that neglect of phase-dispersive processes will lead to unrealistic predictions of NAPL behavior in the vadose zone.

INTRODUCTION

The process of solute dispersion - the spreading of a plume of a dissolved chemical species during advective transport - is of interest in many areas of subsurface flow. Examples include characterization of flow systems through tracer tests, migration of contaminants in groundwater, enhanced oil recovery, geothermal energy production, gas production and storage, solution mining, and geochemical evolution of natural hydrothermal systems. The fundamental mechanism causing dispersion is a random component in magnitude and direction of seepage velocities in porous and fractured media, caused by the irregular geometry of the void space on spatial scales ranging from pore level to regional-scale heterogeneities. The phenomenon of dispersion has been described, with considerable success, as being analogous to Fickian (molecular) diffusion (Scheidegger, 1954, 1974; de Marsily, 1986), although in recent years compelling evidence has been accumulated that the diffusion analogue is of limited applicability in field situations, where dispersivities appear to increase with time and distance of solute transport (de Marsily, 1986; Gelhar et al., 1992). This "scale effect" on dispersivities is not fully understood at present; it seems to be related to the fact that in natural media heterogeneity is present over a broad range of scales (Wheatcraft and Cushman, 1991; Sudicky and Huyakorn, 1991).

In multiphase flow another kind of dispersion process may occur which is also of considerable practical importance in many engineering applications, yet has received only rather limited study. Consider a situation where a fluid phase invades a region in which other fluid phases are present that are not miscible with the invading phase. The

invading phase will then displace some of the resident fluid, and in doing so may disperse longitudinally as well as transversally due to medium heterogeneities and anisotropies, and flow instabilities. Examples of such immiscible or partially miscible displacements are many, including infiltration of water into the vadose zone (displacing soil gas), infiltration of a non-aqueous phase liquid (NAPL; displacing soil gas or water), injection of gas into aquifers for storage purposes, injection of water into vapor-dominated geothermal reservoirs (displacing steam), and many enhanced oil recovery processes, such as water flooding, steam flooding, chemical flooding, and carbon dioxide flooding. To be sure, in such multiphase flow processes "conventional" solute dispersion will also occur within any of the flowing phases, much as solute dispersion occurs in single-phase flow (Sahimi et al., 1986). An additional dispersion process of a different kind will develop, however, in that an invading plume of immiscible fluid phase will not propagate as an invariant shape, but will spread in space and time. We will refer to this process as "phase dispersion," to distinguish it from the conventional solute (miscible) dispersion.

An extreme example of phase dispersion is fingering of an invading phase that arises from an interplay between medium heterogeneity and hydrodynamic instability due to viscosity or density contrast. The displacement of soil gas by water infiltrating into the vadose zone is a gravitationally unstable process and may result in a highly dispersed displacement front where water fingers bypass much of the soil volume (Glass et al., 1989, 1991; Kung, 1990). A similar gravitational instability arises when a NAPL invades the vadose zone, or when a dense NAPL (DNAPL) sinks below the water table. Injection of water into vapor zones in geothermal reservoirs is a gravitationally unstable process (Pruess, 1991), as is the release of gas from strata below the water table in operations such as gas or compressed air storage, or in corrosive gas release from deeply buried nuclear wastes. Viscous instabilities are present in many oil recovery operations, where the displacing phase such as water, steam or gas is less viscous than the resident oil, resulting in highly dispersed displacement fronts.

In this paper we propose an approximate continuum-type approach for describing phase dispersion, in analogy to the description of solute dispersion as Fickian diffusion. The formulation developed here is specialized to the problem of gravity-driven buoyancy flows, such as downward migration (infiltration) of a denser phase, or upward flow of a lighter phase; however, we believe that our approach should be applicable to more general multiphase flow processes. Current mathematical models of multiphase flows capture phase-dispersive processes only when the medium heterogeneities causing such dispersion are described explicitly. This is completely analogous to the situation in solute transport, where no dispersive term is needed when heterogeneities are modeled explicitly; dispersion then arises from the "true" detailed velocity structure (Dagan, 1988; Thompson, 1991). Explicit characterization and modeling is feasible for "large-scale" heterogeneities (with dimensions larger than or equal to grid block sizes), but is impractical for small-scale features of sub-grid block dimensions. A description of phase dispersion by means of explicit modeling of small-scale heterogeneities is limited to numerical experiments with computer-generated heterogeneity structure (Espedal et al., 1991; Kueper and Frind, 1991; Polmann et al., 1991).

Neglect of phase-dispersive mechanisms in the governing equations for multiphase flow may lead to completely unrealistic flow predictions (Pruess, 1991b). For example, gravity-driven infiltration of a dense phase will be predicted to proceed as an essentially straight downward flow when ignoring medium heterogeneities such as small-scale laminations and layering, embedded clay lenses, or irregularities of fractures or fracture networks. (In anisotropic media the direction of gravity-driven flow may deviate from the vertical, but infiltration from a localized source in a homogeneous anisotropic medium would still be predicted to occur as a very narrow plume.) Medium heterogeneities would tend to partially divert flows laterally, in a manner akin to transversal dispersion. An example of such behavior was reported from field experiments at the Borden Site, Ontario, where PCE was allowed to infiltrate into the ground from a point source

(Poulsen and Kueper, 1992). Through subsequent excavation the experimenters determined that the PCE plumes spread horizontally as they descended, reaching horizontal extents of from 0.5 to 2.0 m over an infiltration depth of 2 - 3 m. Soil heterogeneity consisted of millimeter-size laminations with subtle variations in texture, color, and grain size. Numerical experiments have also shown that the main effect of small-scale heterogeneity is a broadening of an infiltrating liquid plume (Kueper and Frind, 1991; Polmann et al. 1991). A continuum model of phase dispersion as proposed here offers a simple means to capture essential effects of such heterogeneity in an approximate fashion, without necessitating a highly detailed description of multiphase flow with explicit representation of heterogeneities that would be impractical for ''real'' systems.

Partial justification for a continuum description of phase dispersion is provided by the recent work of Espedal et al. (1991). These authors investigated two-phase immiscible displacement in two-dimensional domains with stochastic permeability distribution. They performed high-resolution numerical simulations of such displacements to obtain a detailed explicit description of the displacement fronts. Through spatial averaging they then derived a PDE for average saturation. This PDE turned out to be similar in form to the original (microscopic) saturation equation, but included an additional phase-dispersive term. They then obtained solutions for the space-averaged saturation equation by numerical simulation on coarse grids, and were able to show that these approximated well the average longitudinal dispersion of the displacement fronts seen in the high-resolution simulations. It is perhaps not surprising that the process of spatial averaging, whether directly applied to the microscopic saturation equation, or applied to the solution of the microscopic equation, leads to similar results. It is noteworthy, however, that the additional term arising in the space-averaged equation is dispersive in nature, i.e., it corresponds to a flux proportional to $- \mathbf{D} * \nabla S$, where S is the saturation of the invading phase, and $\mathbf{D}$ is a second-order tensor.

In some cases fingering instability in immiscible displacement may be so severe as to prohibit any approximate treatment as a continuum-type dispersion process. An example may be the strong, persistent fingering of water infiltrating into a coarse stratum from an overlying fine-grained zone of low permeability (Glass et al., 1989, 1991). Furthermore, the description of dispersion as a Fickian diffusion process is approximate and of limited validity, even under generally favorable conditions. Nonetheless we expect that in many situations a treatment of phase dispersion by a Fickian diffusion analogue may be a useful approximation. It will likely provide an improvement over existing descriptions of multiphase flows, which make no explicit allowance for phase dispersion at all. Complete absence of phase-dispersive processes can lead to severe errors especially in space-discretized numerical models (Brand et al., 1990; Pruess, 1991b).

It is the purpose of this paper to introduce what we believe to be a plausible mathematical model for multiphase dispersion. To establish a reference case and introduce our notation we begin by briefly summarizing the conventional formulation of solute dispersion in single phase flow. Subsequently we introduce our proposed formulation for phase dispersion. Although applicable to more general processes of immiscible displacements, the treatment in this paper focusses on gravity-dominated flows, such as downflow of a dense phase, or upflow of a light phase. An interesting perspective on phase dispersion is gained by comparison with "physical" dispersion from capillary forces, and by the familiar "numerical" dispersion that arises from a space-discretized treatment of continuum flow processes. Our dispersion model is illustrated by means of applications to problems of water and NAPL infiltration, and geothermal injection. The range of validity of the model has not yet been evaluated. This will require comparison with laboratory and field observations, and computer simulations of two-phase immiscible displacement that represent medium heterogeneity and anisotropy in full explicit detail. Work along these lines is in progress and will be reported elsewhere.

SOLUTE DISPERSION

The conventional treatment of dispersion conceptualizes this process in analogy to Fickian diffusion, described by the customary convection-dispersion equation (de Marsily, 1986)

$$\phi \frac{\partial C}{\partial t} = \text{div}\,(\mathbf{D}\nabla C - C\mathbf{u}) \tag{1}$$

where ϕ is porosity, C is solute concentration, $\mathbf{D}$ is the dispersion tensor, and $\mathbf{u}$ is the volumetric flux (Darcy velocity) of the solution. The solute mass flux

$$\mathbf{F}_{cd} = C\mathbf{u} - \mathbf{D}\nabla C \tag{2}$$

includes a convective term

$$\mathbf{F}_C = C\mathbf{u} \tag{3}$$

and a diffusive-dispersive term

$$\mathbf{F}_d = -\mathbf{D}\nabla C \tag{4}$$

The dispersion tensor is written

$$\mathbf{D} = D_T\mathbf{I} + \frac{D_L - D_T}{u^2}\,\mathbf{u}\,\mathbf{u} \tag{5}$$

with the transversal and longitudinal dispersion coefficients given by, respectively,

$$D_T = \phi d + \alpha_T u \tag{6a}$$

$$D_L = \phi d + \alpha_L u \tag{6b}$$

The first term in Eqs. (6a,b) represents molecular diffusion, while the second term represents hydrodynamic dispersion. The coefficients α_T and α_L have units of length and are customarily called dispersivities.

PHASE DISPERSION

Let us consider a simplified situation of two-phase flow that is applicable to many infiltration problems. A liquid phase such as water or a non-aqueous phase liquid (NAPL) is assumed to infiltrate into the vadose zone and to immiscibly displace a ''passive'' gas phase with negligible pressure buildup in the latter. Liquid volume flux (Darcy velocity) is then given by

$$\mathbf{u}_l = -k \frac{k_{rl}}{\mu_l}(\nabla P_{cap} - \rho_l \mathbf{g}) \tag{7}$$

where k and k_{rl} are, respectively, absolute and relative permeability, μ_l is viscosity, P_{cap} is capillary pressure, ρ_l is liquid density, and **g** is acceleration of gravity. Neglecting phase change processes (evaporation and condensation) and assuming constant liquid density, a liquid phase volume balance can be written as

$$\phi \frac{\partial S_l}{\partial t} = -\operatorname{div} \mathbf{u}_l \tag{8}$$

where S_l is liquid saturation. The flux expression Eq. (7) can be rewritten in a form that is analogous to the convective-dispersive solute flux of Eq. (2)

$$\mathbf{u}_l = S_l \hat{\mathbf{v}} - \mathbf{D}_{cap} \cdot \nabla S_l \tag{9}$$

where

$$\hat{\mathbf{v}} = k \frac{k_{rl}}{\mu_l S_l} \rho_l \mathbf{g} \tag{10}$$

plays the role of advection velocity, and

$$\mathbf{D}_{cap} = k \frac{k_{rl}}{\mu_l} \frac{dP_{cap}}{dS_l} \mathbf{I} = \frac{1}{\rho_l g} \hat{\mathbf{v}} \frac{dP_{cap}}{d \ln S_l} \mathbf{I} \tag{11}$$

is a tensor that represents capillary effects.

We mention in passing that an easy improvement of Eqs. (7) through (11) can be achieved by replacing ρ_l with $(\rho_l - \rho_g)$, to account for the buoyancy effect of the displaced phase. For water infiltration under ambient conditions in the vadose zone the density contrast between displacing and displaced phase is approximately 1000, so that this correction amounts to an insignificant value of approximately 0.1 %; however, for infiltration of dense NAPL below the water table this correction is essential, as the density of invading DNAPL is of the same order as that of the displaced water.

From Eq. (10) we note that $\hat{\mathbf{v}}S_l$ is the Darcy velocity due to gravity-driven flow, so that $\hat{\mathbf{v}}$ may be interpreted as a velocity of liquid phase propagation that is enhanced due to the fact that liquid is present at a saturation $S_l < 1$. $\mathbf{D}_{cap}$ can be interpreted as a tensor of ''phase dispersion'' due to capillary action. Capillary phase dispersion is isotropic, and by comparison with Eq. (6) the corresponding dispersivity may be identified as

$$\hat{\alpha}_{cap} = \frac{1}{\rho_l g} \frac{dP_{cap}}{d \ln S_l} \tag{12}$$

While solute dispersivities are generally considered constants independent of solute concentration, the capillary dispersivity of an immiscible phase infiltrating under gravity is seen to generally vary with liquid phase saturation S_l, being independent of S_l only in the special circumstance where $P_{cap} \sim \ln S_l$.

With these definitions, the volume balance equation (8) can be rewritten in the form of a convection-dispersion equation for saturation, in complete analogy to Eq. (1) for solute concentration. Inserting Eq. (9) into Eq. (8) we have

$$\phi \frac{\partial S_l}{\partial t} = \mathrm{div}(\mathbf{D}_{cap} \nabla S_l - S_l \hat{\mathbf{v}}) \tag{13}$$

Note that so far we have only recast Eqs. (7) and (8) in different form, without any changes in substance. Exploiting the formal analogy of Eq. (13) with Eq. (1) we now propose that effects of hydrodynamic dispersion of an invading liquid phase from medium heterogeneities, anisotropies, and flow instabilities may be approximated by a

suitable extension of the capillary dispersion tensor. In analogy to Eqs. (5) and (6) we write

$$\mathbf{D} = \mathbf{D}_{cap} + \mathbf{D}_{dis}$$

$$= D_T \mathbf{I} + \frac{D_L - D_T}{\hat{v}^2} \hat{\mathbf{v}}\,\hat{\mathbf{v}} \tag{14}$$

with the transversal and longitudinal elements of the phase dispersion tensor given by

$$D_T = (\hat{\alpha}_{cap} + \hat{\alpha}_T)\hat{v} \tag{15a}$$

$$D_L = (\hat{\alpha}_{cap} + \hat{\alpha}_L)\hat{v} \tag{15b}$$

Exploiting the identity $\hat{\mathbf{v}}/\hat{v} = \mathbf{g}/g$, the proposed form Eq. (14) of the phase dispersion tensor for gravity-driven infiltration processes may be rewritten as

$$\mathbf{D} = D_T \mathbf{I} + \frac{D_L - D_T}{g^2} \mathbf{g}\,\mathbf{g} \tag{16}$$

Physically it is to be expected that the transversal and longitudinal phase dispersivities $\hat{\alpha}_T$ and $\hat{\alpha}_L$ introduced in Eqs. (15a,b) should not be constants but should depend on liquid saturation. The reason for this is that, at different saturation levels, different portions of the pore space with generally different geometry and heterogeneity will participate in liquid flow (Sahimi et al., 1986; Espedal et al., 1991). At present we have no information on the nature and strength of the dependence of phase dispersivities on saturation.

The phase-dispersive mass flux may be written

$$\mathbf{F}_{l,dis} = -\rho_l \mathbf{D}_{dis} \nabla S_l \tag{17}$$

Inserting from Eqs. (10), (15), and (16), this becomes

$$\mathbf{F}_{l,dis} = -\frac{k\rho_l}{\mu_l} (\hat{\alpha}_T \rho_l g) \frac{k_{rl}}{S_l} \nabla S_l$$

$$+\frac{k\rho_l}{\mu_l} (\hat{\alpha}_L - \hat{\alpha}_T) \rho_l g \frac{k_{rl}}{S_l} \frac{\partial S_l}{\partial z} \cdot \frac{\mathbf{g}}{g} \tag{18}$$

where we have introduced a z-coordinate axis pointing vertically upward. These equations essentially complete our formal development of the phase dispersion process during infiltration. To further elucidate the physical ''meaning'' of our proposed formulation let us assume for the moment that phase dispersivities are only weakly dependent on saturation. Introducing an ''average'' constant phase dispersivity $\hat{\alpha}_0$, Eqs. (15a,b) can be rewritten, using Eq. (12), as

$$D_{T,L} = \frac{1}{\rho_l g}\,\hat{v}\,\frac{d}{d\ln S_l}(P_{cap} + \hat{\alpha}_{o_{T,L}}\rho_l g \ln S_l) \tag{19}$$

Eq. (19) indicates that in our proposed formulation phase-dispersive effects can be thought of, in an approximate way, as equivalent to an additional capillary pressure which is proportional to the logarithm of phase saturation. Note that this ''dispersive'' capillary pressure will in general be anisotropic, presumably being weaker in the horizontal than in the vertical direction, as we expect $\hat{\alpha}_{0,T} < \hat{\alpha}_{0,L}$. Further note that it is negative regardless of whether the invading phase is wetting or non-wetting, so it will always tend to spread infiltrating plumes. The close formal correspondence between capillary and phase-dispersive effects expressed in Eq. (19) may be useful for evaluating conditions under which one or the other effect would dominate. Generally speaking, we expect phase-dispersive mechanisms to be most important when capillary pressures are weak.

Additional insight can be gained from further elaboration of the liquid volume balance Eq. (8). Considering only the gravity flow term in Eq. (7), and again neglecting (small) variations in density and viscosity, we have (Pruess, 1991b)

$$\frac{\partial S_l}{\partial t} = \left[\frac{k\rho_l g}{\phi\mu_l}\,\frac{dk_{rl}}{dS_l}\right]\frac{\partial S_l}{\partial z} \tag{20}$$

which is a first-order hyperbolic equation with traveling wave solutions of the form $S(z,t) = f(z+tv/\phi)$, where v/ϕ given by

$$\frac{v}{\phi} = \frac{k\rho_l}{\phi\mu_l}\,\frac{dk_{rl}}{dS_l}\,g \tag{21}$$

is the propagation velocity of saturation disturbances. Comparing Eqs. (21) and (10), the relationship between v and $\hat{v}$ is

$$\mathbf{v} = \hat{\mathbf{v}} \frac{d \ln k_{rl}}{d \ln S_l} \tag{22}$$

Eq. (20) suggests that it may be more appropriate to formulate phase dispersion in terms of v rather than $\hat{v}$. To do this we rewrite Eqs. (15a,b) with reference to v as follows

$$D_T = (\alpha_{cap} + \alpha_T)\, v \tag{23a}$$

$$D_L = (\alpha_{cap} + \alpha_L)\, v \tag{23b}$$

so that, from $\alpha v = \hat{\alpha}\hat{v}$,

$$\alpha = \hat{\alpha} \frac{d \ln S_l}{d \ln k_{rl}} \tag{24}$$

Capillary dispersivity with respect to v is then, from Eqs. (12) and (24),

$$\alpha_{cap} = \frac{1}{\rho_l g} \frac{dP_{cap}}{d \ln k_{rl}} \tag{25}$$

and Eq. (18) for the phase-dispersive mass flux becomes

$$\mathbf{F}_{l,dis} = -\frac{k\rho_l}{\mu_l} (\alpha_T \rho_l g) \nabla k_{rl} + \frac{k\rho_l}{\mu_l} (\alpha_L - \alpha_T)\, \rho_l g \frac{\partial k_{rl}}{\partial z} \frac{\mathbf{g}}{g} \tag{26}$$

To relate the v-based dispersion formulation to capillary effects, we proceed as in the derivation of Eq. (19). Introducing an average constant α_0, independent of S_l, hence k_{rl}, Eqs. (23) can be expressed as

$$D = \frac{1}{\rho_l g}\, v \frac{d}{d \ln k_{rl}} (P_{cap} + \alpha_o \rho_l g \ln k_{rl}) \tag{27}$$

The $\hat{v}$ and v-based formulations, Eqs. (18) and (26), or (19) and (27), are completely equivalent. The choice of a reference velocity for phase dispersion only affects the dependence of dispersivities on saturation, see Eq. (24). It would be desirable to choose the reference velocity in such a way that dispersivities depend on saturation as weakly as possible. Intuitively one expects that the v-based formulation is preferred, but this is speculative at present.

FURTHER PERSPECTIVE ON PHASE DISPERSION

An interesting perspective on our formulation of phase dispersion can be gained by considering an exponential relationship between relative permeability and capillary pressure,

$$k_{rl} = \exp\left(\beta \frac{P_{cap}}{\rho_l g}\right) \tag{28}$$

This is of semi-quantitative validity in many media and is of special interest because it leads to simple quasi-linear models (Pullan, 1990). The parameter β has units of inverse length, and is often referred to as ''sorptive number''. From Eq. (27) the dispersive addition to capillary pressure then takes on the approximate form

$$P_o^{dis} = \alpha_o \beta P_{cap} \tag{29}$$

so that the effect of phase dispersion would be approximately equivalent to multiplying the strength of capillary pressure by a factor $(1 + \alpha_0\beta)$. Alternatively, an effective capillary dispersivity can be calculated from Eqs. (25) and (28) as $\alpha_{cap} = 1/\beta$. This indicates that capillarity will dominate when $1/\beta >> \alpha_L$ or α_T, while phase dispersion will dominate in the opposite circumstances, $\beta >> \alpha_l$ or α_T. Fine-grained media have small β, hence are likely to be capillary-dominated, while in coarse media β is large and phase dispersion may dominate.

Another interesting comparison can be made with "numerical" phase dispersion effects that arise in numerical simulations of immiscible displacements. Analyzing finite-difference approximations of gravity-driven liquid flow in two-dimensional vertical sections, Pruess (1991b) showed that the finite space discretization gives rise to artificial "numerical" phase dispersion effects which generally are anisotropic, and mathematically are equivalent to an "effective grid capillary pressure," given by

$$P_{cap}^{grid} = C \rho_l g \ln k_{rl} \tag{30}$$

The coefficients C have units of length and can be thought of as "numerical phase dispersivities" (compare Eqs. 25, 27). The analysis presented in (Pruess, 1991b) shows that numerical dispersivities are constants, independent of saturation, whose magnitude is of the order of the grid spacing. Numerical dispersion is generally anisotropic. It depends on the orientation of the computational grid relative to the vertical, as well as on the finite difference approximation used. Table 1 (from Pruess, 1991b) lists numerical phase dispersivities for parallel and diagonal vertical grids of square blocks with side length h (see Fig. 1), and for five- and nine-point finite difference schemes (Fig. 2; Forsythe and Wasow, 1960; Yanosik and McCracken, 1979).

Table 1. Transversal and longitudinal numerical phase dispersivities C_T and C_L in vertical grids (from Pruess, 1991b).

Grid	C_T	C_L
parallel 5-point	0	h/2
9-point	h/6	h/2
diagonal 5-point	$h/(2\sqrt{2})$	$h/(2\sqrt{2})$
9-point	$h/(3\sqrt{2})$	$(h\sqrt{2})/3$

It is interesting to note that the numerical dispersion effects represented by Eq. (30) are identical in form to the approximate expression Eq. (27) for our proposed model for phase dispersion. We believe that this correspondence is more than a fortuitous coincidence. Finite-difference modeling implies that fluids upon entering a grid block "instantaneously" spread and mix throughout the grid block volume. This process bears a close similarity to the "mixing cell" approach in which tracer migration is modeled as proceeding through a series of finite-volume compartments (Nir and Kirk, 1982), within each of which fluids are completely mixed in the sense of a "well-stirred" reactor. In the present context our interest is in phase dispersion rather than solute dispersion, and the instantaneous spreading or mixing within a finite-volume block would refer to an immiscible fluid phase rather than to dissolved solute. The finite-compartment model has an intuitive appeal, and the close formal correspondence between numerical phase dispersion in finite difference models and our proposed model for physical phase dispersion seems to lend additional support to the latter.

NUMERICAL SIMULATION

We have incorporated the Fickian model for phase dispersion into our multiphase multicomponent simulators TOUGH2† (Pruess, 1987, 1991a) and STMVOC (Falta et al., 1992). To derive a finite difference expression for the phase-dispersive flux, Eq. (26), we introduce a Cartesian coordinate system ($\mathbf{e}_x$, $\mathbf{e}_y$, $\mathbf{e}_z$), with unit vectors $\mathbf{e}_x$ and $\mathbf{e}_y$ being horizontal, and $\mathbf{e}_z$ pointing vertically upward. Eq. (26) can be rewritten as

$$\mathbf{F}_{l,dis} = -k \frac{\rho_l}{\mu_l} \rho_l g \left[\mathbf{e}_x \alpha_T \frac{\partial k_{rl}}{\partial x} + \mathbf{e}_y \alpha_T \frac{\partial k_{rl}}{\partial y} + \mathbf{e}_z \alpha_L \frac{\partial k_{rl}}{\partial z} \right] \tag{31}$$

Discretization of Eq. (31) is accomplished by introducing first-order finite differences for the derivatives of liquid relative permeability. Appropriate weighting schemes are

† Available from: Energy Science and Technology Software Center (ESTSC), P.O. Box 1020, Oak Ridge, TN 37831

required for the coefficients multiplying the gradients of relative permeability. The phase dispersivities α_T and α_L may generally depend on saturation but were assumed to be constants in this work; thus they pose no issue with respect to finite difference approximation. The factors in front of the parentheses are "interface quantities," which generally depend on conditions in both grid blocks between which flow is taking place. The customary TOUGH2 options are employed here, including harmonic or upstream weighting for absolute permeability, upstream weighting for the group (ρ_l / μ_l), and averaging for the group $(\rho_l g)$.

Another subtle point deserves mentioning. The implementation of Eq. (31) as it stands may give rise to dispersive flux in a direction opposite to the general advective flow. Indeed, for $\partial k_{rl}/\partial z < 0$ dispersive flux will be upward, opposing gravity. This unphysical behavior is analogous to the well-known phenomenon of upstream migration in conventional models of Fickian solute dispersion (de Marsily, 1986). In our finite-difference implementation of Eq. (31) we avoid unphysical flows by testing for the sign of $\partial k_{rl}/\partial z$, and permitting dispersive flux only in the downward and horizontal directions.

In this paper we consider dispersivities to be constants, independent of saturation. Under these conditions the capillary analogue Eq. (27) is not an approximation but is strictly valid. It offers an alternative approach for finite-difference implementation of Fickian phase dispersion which conceptually is extremely simple. All that is needed is addition of a phase-dispersive capillary pressure,

$$P_{dis} = \alpha \rho_l g \ln k_{rl} \tag{32}$$

where $\alpha = \alpha_T$ for horizontal flow connections, and $\alpha = \alpha_L$ for vertical flow connections.

We also implemented the phase dispersion by means of the equivalent capillary pressure given in Eq. (32). Through test calculations for many different saturation conditions we verified that both formulations yield identical fluxes. However, we found that the capillary pressure formulation has serious drawbacks in practical applications. It

diverges as relative permeability approaches zero, and generally tends to be more strongly non-linear, so that it is subject to more severe space truncation errors when calculating finite-difference fluxes between grid blocks that have a finite difference in saturations. The ∇k_{rl} based formulation, Eq. (31), lends itself well to finite-difference approximation, and it was used for all calculations presented in this paper.

APPLICATIONS

We now present illustrative applications of the Fickian phase dispersion model. The problems considered include infiltration of water and trichloroethene (TCE) into the vadose zone, and water injection into low-pressure vapor zones in geothermal reservoirs.

By analogy to solute dispersion in single-phase miscible flow one may expect longitudinal phase dispersivity to be larger than transversal phase dispersivity. However, the latter will have a more dramatic impact on flow behavior in multiphase infiltration problems. Indeed, longitudinal (vertical) phase dispersion will only modify the predominant downward advective migration, while transversal dispersion will lead to a qualitatively new behavior, namely, a lateral (horizontal) spreading of infiltration plumes in isotropic media where gravity-driven advective flow is strictly downward. The simplest problem that can serve to illustrate the phenomena is water infiltration in the vadose zone from a localized source, such as an irrigation line. Subsequently we proceed to the practically significant and more difficult three-phase problem of phase dispersion during infiltration of spilled TCE. Our final example concerns water injection into superheated vapor zones. This is an important problem in the management of vapor-dominated geothermal reservoirs, which involves immiscible displacement coupled with strong heat transfer and phase change processes.

WATER INFILTRATION INTO THE VADOSE ZONE

We consider water infiltration into the vadose zone. The model system (Fig. 3) is a two-dimensional vertical (X-Z) section of 1 m thickness. Space discretization is made into square blocks of 2.5 m side length. The water table is at a depth of 37.5 m. For relative permeability we use the formulation given by Corey (1954). A reduced liquid saturation S^* is defined as

$$S^* = (S_l - S_{wr})/(1 - S_{wr} - S_{gr}) \tag{33}$$

with S_{wr} and S_{gr} being irreducible liquid and gas saturation, respectively. Liquid and gas relative permeabilities are

$$k_{rl} = (S^*)^4 \tag{34}$$

$$k_{rg} = (1 - S^*)^2(1 - [S^*]^2) \tag{35}$$

Capillary pressures were neglected to better highlight effects of phase dispersion. The problem parameters for this and the other illustrative problems are summarized in Table 2.

Prior to start of infiltration the system is run to static gravity-capillary equilibrium, using a two-phase treatment that accounts for the small vertical pressure gradient corresponding to gravity equilibrium for soil gas. Equilibrated gas pressures and liquid saturations are then held constant at the right boundary, and water is infiltrated at a rate of .05 kg/s into the upper left hand grid block. The left boundary is modeled as a symmetry plane, using ''no flow'' boundary conditions. Several cases were run using different values for transversal phase dispersivity, and different finite difference schemes.

A calculation without phase dispersion shows the behavior that is expected in a homogeneous isotropic medium. At an infiltration rate much below maximum gravity-driven flow, and with no capillary pressure, there is no driving force for lateral flow. A simulation with a standard 5-point finite difference scheme produces a narrow downward slumping plume that remains confined to the first (leftmost) column of grid blocks

(results not shown). Recall from Table 1 that five-point differencing in a ''parallel'' grid that is aligned with horizontal and vertical directions has the unique property that transversal numerical phase dispersion vanishes. Thus there is neither a physical nor a numerical effect that could give rise to a broadening of the plume. Addition of a transversal phase dispersivity of $\alpha_T = 0.2$ m causes a lateral broadening of the infiltration plume (Fig. 4) as expected, which becomes very pronounced when the system is run to steady state (Fig. 5). Steady state conditions are approached quickly in the upper interior portion of the plume, while the outer regions with only slightly elevated liquid saturation continue to spread on a very slow time scale. An approximate doubling of the transversal phase dispersivity has only modest impact on the inner high-saturation region of the plume, while strongly affecting the peripheral regions of slightly elevated liquid saturation. Fig. 6 shows the steady-state plume for a transversal phase dispersivity of $\alpha_T = 0.4167$ m, a value that was chosen to permit a direct comparison with the steady-state plume for 9-point differencing and no phase dispersion in Fig. 7. Note that, according to Table 1, both calculations have the same numerical (and no physical) longitudinal phase dispersivity, while the numerical transversal phase dispersivity in the 9-point calculation of $C_T = 2.5/6 = 0.4167$ m is equal to the physical phase dispersivity in the 5-point calculation.

Based on the equivalence between numerical and physical phase dispersion discussed above we expect that both infiltration plumes should be identical. Inspection of Figs. 6 and 7 shows that, for the most part, the saturation contours agree, but there are also significant differences. In the 9-point scheme no portion of the plume extends upward beyond the main diagonal of the grid, while the physical phase dispersion effect leads to significant lateral spreading above the diagonal. The main reason for the lack of closer agreement is in the upper boundary condition in the 9-point differencing scheme. Indeed, the 9-point approximation is violated in the top row of grid blocks which have no flow connections going upward. The derivation of the numerical phase dispersivities as

Table 2. Parameters used in simulations

	water infiltration	TCE infiltration	geothermal injection
permeability (m^2)	15.8×10^{-12}	10×10^{-12}	10×10^{-12}
porosity	.35	.35	.05
soil (rock) density (kg/m^3)	†	†	2600.
specific heat (J/kg°C)	†	†	1000.
thermal conductivity (W/m°C)	†	†	2.1
relative permeability	Eqs. 33-35	Eqs. 36-38	Eqs. 33-35
irreducible water saturation	.10	.15	.30
irreducible gas saturation	.01	.01	.05
irreducible NAPL saturation	-	.05	-
exponent	-	3.0	-
initial conditions:			
temperature (°C)	20.0	20.0	240.
pressure (bar)	1.0	1.013	10.
water saturation	.10	.15	0
injection specifications:			
water rate (kg/s)	.05	-	.01
water enthalpy (kJ/kg)	†	-	125.8
TCE rate (kg/s)	-	$.7687 \times 10^{-3}$	-

† isothermal problem, no thermal data needed.

given in (Pruess, 1991b) is only valid in the interior of the flow domain, where grid blocks can receive downward flow. This suggests that a better confirmation of the correspondence between numerical and physical phase dispersion should be possible by eliminating the effects of the upper boundary. Accordingly, we initialized a 9-point simulation from the upper (top row of grid blocks) boundary conditions obtained for the steady state with transversal phase dispersivity of $\alpha_T = 0.4167$ m. The resulting steady state (Fig. 8) agrees quite closely with the steady state for physical phase dispersion in the 5-point grid, Fig. 6. Remaining small discrepancies are believed to be caused by higher order space derivative terms (third order and beyond) which are different in the two formulations.

TCE SPILL

Spills or leaks of non-aqueous phase liquids, such as solvents or fuel oils, have frequently occurred at low rates in near-surface environments. The present problem assumes that a quantity of 465 kg of TCE, corresponding to two barrels, is spilled over a 7-day period. Infiltration into a homogeneous soil column of 10 Darcy permeability occurs from a point-like source of 15 cm diameter. The water table is at a depth of 40 m. There is no infiltration of water, and the entire unsaturated zone is initialized at an irreducible water saturation of 15%. Three-phase relative permeabilities are represented by a slightly modified version of Stone's first method (Stone, 1970). For water, gas, and NAPL-phases we have, respectively,

$$k_{rw} = \left[\frac{S_w - S_{wr}}{1 - S_{wr}}\right]^n \qquad (36)$$

$$k_{rg} = \left[\frac{S_g - S_{gr}}{1 - S_{wr}}\right]^n \qquad (37)$$

$$k_{nr} = \left[\frac{1 - S_g - S_w - S_{nr}}{1 - S_g - S_{wr} - S_{nr}}\right]\left[\frac{1 - S_{wr} - S_{nr}}{1 - S_w - S_{nr}}\right]\left[\frac{(1 - S_g - S_{wr} - S_{nr})(1 - S_w)}{(1 - S_{wr})}\right]^n \qquad (38)$$

where n is the exponent (Table 2), and S_{wr}, S_{gr} , and S_{nr} represent, respectively, irreducible saturation of water, gas, and NAPL phases. Water-gas capillary pressures are represented by van Genuchten's formulation (van Genuchten, 1980), written in the form

$$P_{cgw} = -\frac{\rho_w g}{a_{gw}}\left[\left[\frac{1-S_m}{S_w-S_m}\right]^{\nu/(\nu-1)} - 1\right]^{1/\nu} \qquad (39)$$

with parameters a_{gw} = 5.0 m^{-1}, S_m = 0, and ν = 1.84. Capillary pressure between the NAPL and gas phases is assumed negligibly small. The behavior of the contaminant is modeled in a two-dimensional radially symmetric (R-Z) system, with constant pressure conditions maintained at the land surface. Radial grid increments are small near the spill point, increasing logarithmically to the large outer radius of 300 m, see Fig. 9. Additional problem specifications are given in Table 2.

The NAPL behavior during and subsequent to the spill event is simulated with the STMVOC code, an offshoot of TOUGH developed by Falta et al. (1992a, b) for the flow of three immiscible phases. STMVOC represents full multi-phase partitioning (vaporization and aqueous dissolution) of the NAPL. It includes advective flow in all three phases, as well as multicomponent diffusion in the gas phase. Adsorption of the NAPL to the porous medium can also be accounted for, although it was assumed negligible in the present case. Fig. 10 shows simulated saturations of free-phase TCE at the end of the 7-day spill period, without any phase dispersion. It is seen that flow of the NAPL phase in the unsaturated zone is straight downward, as was to be expected. Indeed, the only driving force for lateral flow is provided by the increase in soil gas pressure due to the invasion of the TCE plume. This increase and associated lateral TCE migration are very small, because of the very small viscosity of the soil gas that is being displaced. The situation is very different once the plume reaches the water table. Water viscosity is larger than TCE viscosity at ambient temperature, so that non-negligible pressurization occurs as TCE displaces water. This provides a driving force which causes the TCE plume to spread laterally. The effect is amplified by capillary suction effects, which drive

water towards the region of diminished water saturation in the TCE plume.

The fate of the contaminant plume is entirely different when transversal phase dispersion is included. Figures 11 and 12 show simulated saturations of free-phase TCE at the end of the 7-day spill period, for transversal phase dispersivities of α_T = .002 m and α_T = .02 m, respectively. The plume now spreads not only downward but also laterally in the unsaturated zone. The lateral spreading is stronger for larger transversal dispersivity, as expected, but even for a "small" dispersivity of .002 m the spreading is very significant. Because of the radial flow geometry, the rather modest broadening of the plume to approximately 1 m diameter, as compared to the 0.15 m diameter of the spill, offers sufficient volume to retain all of the free-phase TCE within the unsaturated zone, above the water table.

The different plume configurations with and without phase dispersion at the end of the spill period make for very different behavior after the spill has terminated, when the flow system is left to its internal driving forces. The results for a 5-year period following the spill are summarized in Table 3.

Table 3. TCE inventory following a spill of 465 kg over 7 days.

	time = 7 days			time = 1 year			time = 5 years		
	no phase dispersion	α_T =.002m	α_T = .02 m	no phase dispersion	α_T =.002m	α_T = .02 m	no phase dispersion	α_T =.002m	α_T = .02 m
free phase	434.1 kg	447.1 kg	451.3 kg	358.3 kg	0.0 kg	11.2 kg	358.3 kg	0.0 kg	0.0 kg
dissolved	13.1 kg	5.7 kg	4.1 kg	34.5 kg	116.7 kg	76.0 kg	23.8 kg	64.4 kg	33.3 kg
gaseous	17.2 kg	11.2 kg	8.2 kg	51.8 kg	233.1 kg	152.0 kg	30.3 kg	128.6 kg	66.6 kg
total	464.4 kg	464.0 kg	463.6 kg	444.6 kg	349.8 kg	239.2 kg	412.4 kg	193.0 kg	99.9 kg

At the end of the spill period (7 days) most of the TCE is present as a free NAPL phase. The amount vaporized into the soil gas phase (and a corresponding amount

dissolved in immobile water) is small, but is larger when phase dispersion is neglected. This is explained by the fact that the non-dispersed plume has a smaller radius and therefore, at approximately equal total volume, has a larger surface area than the dispersed plumes for contacting soil gas. At later times the phase-dispersed plumes are subject to much stronger vaporization. After one year, in the case without phase dispersion approximately 77% of spilled TCE forms a free-phase plume beneath the water table. This plume is not affected by gas phase diffusion and advection; it remains unchanged after 5 years as there is no regional groundwater flow in our system that could dissolve it. The phase-dispersed plumes on the other hand remain in the unsaturated zone where they are subject to very substantial diffusive and advective gas phase flow effects. Due to its proximity to the land surface, a significant amount of TCE is removed from the flow system simply by diffusion into the atmosphere. With increasing transversal phase dispersivity, more of the TCE plume remains close to the ground surface, resulting in stronger decline of TCE inventory from diffusion across the land surface. The vapor migration occurs both by diffusion and by buoyancy-driven gas flow: a column of soil gas containing TCE vapors is heavier than clean air; it flows downward, inducing entry of clean atmospheric air into the soil upstream from the NAPL plume, thus providing for continuing vaporization into the flowing gas stream (Falta et al., 1989). TCE vapors are subject to equilibrium phase partitioning into the aqueous phase. The ratio of dissolved to vaporized TCE inventory in the simulations with phase dispersion is seen to be approximately 0.50 at all times. This particular ratio is somewhat fortuitous, and is explained as follows. From aqueous solubility and vapor pressure of TCE one can calculate that, at a temperature of 20°C, the ratio of partial TCE densities (concentrations) in aqueous and gaseous phases is 2.83. In the present problem, water saturation in the unsaturated zone is .15, so that the ratio of dissolved to vaporized TCE mass in the unsaturated zone is $2.83 \times .15/.85 = 0.50$. In the simulations without phase dispersion additional TCE is dissolved in the aqueous phase below the water table, so that the ratio of dissolved to vaporized TCE is larger.

Although total TCE inventory changes monotonically with tranversal phase dispersivity at all times, TCE inventories in NAPL, aqueous, and gaseous phases show a more complicated behavior. After 1 and 5 years, the amounts of TCE dissolved in the aqueous and vaporized in the gas phase are larger for α_T = .002 m than for α_T = 0 or α_T = .02 m. This is explained by noting that for α_T = .002 m less TCE leaves the flow system by diffusion into the atmosphere as compared to α_T = .02 m, while the larger surface area of the TCE plume for α_T = .002 m enhances diffusive migration away from the NAPL plume, promoting more rapid evaporation.

It is clear from the above discussion that a rather small amount of phase dispersion can completely alter the behavior of NAPL plumes in thick unsaturated zones, both during initial infiltration and also during subsequent multiphase transport processes. This observation suggests that numerical simulations of NAPL flow processes that do not account for effects of ubiquitous small-scale heterogeneity may give completely spurious and unrealistic results.

WATER INJECTION INTO VAPOR-DOMINATED GEOTHERMAL RESERVOIRS

Vapor-dominated geothermal reservoirs are a rare but practically important type of geothermal system. They produce dry steam (usually) that is directly useable for electric power generation. The vapor-dominated fields at The Geysers, California, and Larderello, Italy, have been utilized for power generation for several decades. Fluid withdrawal has caused well flow rates and pressures to decline. Water injection is the chief means by which dwindling fluid reserves can be replenished and a larger fraction of the heat energy stored in the rocks be recovered.

Injection of water into depleted (low pressure) vapor zones gives rise to a complex interplay of fluid flow and heat transfer processes with phase change. The process is gravitationally unstable, and is further complicated by the fractured-porous nature of vapor-dominated reservoirs. Injected water will enter the reservoir primarily through a

number of fractures intercepted by the injection well. The fractures tend to be steeply dipping and form an irregular network. Heterogeneities are expected to be important on all scales from individual fractures to reservoir-scale networks. The unfractured matrix rock has low permeability, of order microdarcies. It provides heat transfer to boil injected water in the fractures, and it can absorb water by means of capillary imbibition and other processes (Pruess and O'Sullivan, 1992; Pruess and Enedy, 1993).

Engineering design of injection systems requires a capability to realistically describe the evolution of boiling plumes of injected water, so that undesirable thermal degradation and liquid interference at production wells may be avoided. In the major fractures capillary effects will be weak, so that water movement will essentially be determined by gravity-driven advective flow within a heterogeneous setting. In a ''conventional'' modeling approach using homogeneous permeability, phase dispersion will arise only from numerical grid effects. In the most commonly used parallel grid with 5-point differencing this numerical dispersion is highly anisotropic (see Table 1), providing no mechanism for lateral (horizontal) spreading of injection plumes. Accordingly, injection plumes take the shape of narrow downward slumping fingers (Lai and Bodvarsson, 1991; Shook and Faulder, 1991, Pruess, 1991b). Inclusion of physical phase dispersion effects provides a mechanism for lateral water migration. This will have an important impact on the area for rock-fluid heat transfer available to the injection plume, and for possible breakthrough of liquid water at production wells.

We have used an idealized two-dimensional vertical section model representing a highly permeable fracture zone to examine phase-dispersive effects during water injection into a low-pressure vapor zone (see Fig. 13). Problem specifications are given in Table 2. Simulated results for injection plumes without allowance for phase dispersion effects in parallel and diagonal 5-point grids are shown in Fig. 14. They exhibit the trends expected from the analysis of numerical dispersivities, Table 1. The parallel grid generates no transversal numerical phase dispersion, and accordingly gives a straight

downward slumping plume. In contrast, the diagonal grid has a transversal numerical phase dispersivity of $h/(2\sqrt{2}) = 3.54$ m, which causes a significant broadening of the plume. A detailed analysis of space discretization errors for this problem was given in (Pruess, 1991b).

Fig. 15 shows an injection plume predicted from a 5-point parallel grid with a phase dispersivity of 1.67 m. The broadening of the plume is entirely due to the physical phase dispersion effect. For comparison we show simulation results obtained with the same grid, but using 9-point differencing and no phase dispersion (Fig. 16). According to Table 1, both simulations have the same total (numerical plus physical) phase dispersivities, both in transversal and longitudinal directions. Inspection of Figs. 15 and 16 shows that the agreement between them is excellent.

DISCUSSION AND CONCLUSIONS

In many applications involving multiphase flow medium heterogeneity is the key to understanding and modeling flow and transport. Heterogeneity in the unsaturated zone typically occurs on a broad range of scales, from "small" (millimeters to meters) to "large" (meters to kilometers). Conceptually, large-scale heterogeneity can be dealt with rather easily; it is accounted for by explicitly discretizing the flow domain and assigning appropriate material properties to the various subdomains. Small-scale heterogeneity poses more difficult problems. Physical and numerical experiments have shown that ever-present and seemingly insignificant heterogeneities down to the millimeter scale can have very strong effects on multiphase flow behavior, especially in the case of NAPL fluids infiltrating in the unsaturated zone (Poulsen and Kueper, 1992; Kueper and Frind, 1991). Clearly, detailed characterization of such small-scale heterogeneity will be impossible for most flow systems of practical interest, and it would be impractical to explicitly account for it in numerical models. Description of multiphase flow in the presence of small-scale heterogeneity then faces a problem completely analogous to the

problem of solute transport in heterogeneous media. This paper proposes to deal with this problem in a similar way, by adding a phenomenological dispersive flux term to the governing equations for multiphase flows.

Whereas in solute transport the quantity being dispersed is solute concentration, the quantity subjected to "phase dispersion" is phase saturation S. Restricting ourselves to gravity-driven infiltration problems, we have recast the multiphase flow equations into the familiar form of the convection-dispersion equation, with capillarity being represented by a dispersion tensor. This tensor is then generalized in analogy to the customary tensor of solute dispersion to include transversal and longitudinal phase dispersion effects. It is shown that the proposed phase dispersion term is analogous to a capillary pressure with strength proportional to the logarithm of liquid relative permeability. Hence, the effective phase-dispersive capillary pressure is always negative, regardless of phase wettabilities. The driving "force" for phase dispersion is provided by relative permeability gradients.

We have derived finite-difference approximations for the phase-dispersive flux, which were coded into our multiphase flow simulators TOUGH2 and STMVOC. Analysis of space truncation errors in the finite difference approximation leads to the identification of grid effects which are equivalent to the proposed "physical" phase dispersion. Calculations for infiltration of water and trichloroethene (TCE) into the vadose zone, and injection of water into depleted vapor-dominated geothermal reservoirs, have demonstrated that the basic effect of phase dispersion is a horizontal broadening of descending liquid plumes. Our simulations have also verified the close correspondence between physical phase dispersion, and numerical phase dispersion which arises as an artefact of space discretization.

We emphasize that our calculations are intended to illustrate typical effects that follow from our proposed model for phase dispersion. Applicable parameter choices and indeed the range of validity for the model are not known at present. Experimental and

modeling studies will be needed to explore the conditions that would permit application of a Fickian diffusion model to phase dispersion, and to establish magnitude and possible saturation dependence of phase dispersivities.

ACKNOWLEDGEMENT

The author gratefully acknowledges the support and hospitality of the Institut fuer Stroemungsmechanik (Dr. Werner Zielke), University of Hanover, Germany, where part of this work was performed. Additional support was provided by the U.S. Department of Energy under Contract No. DE-AC03-76SF00098. Thanks are due to Drs. A. Datta-Gupta, S. Finsterle, I. Javandel, and C.F. Tsang for reviewing the manuscript and suggesting improvements.

REFERENCES

Brand, C. W., Heinemann, J. E. and Aziz, K., The Grid Orientation Effect in Reservoir Simulation, paper SPE-21228, presented at Society of Petroleum Engineers Eleventh Symposium on Reservoir Simulation, Anaheim, CA, February 1991.

Corey, A. T., The Interrelation between Gas and Oil Relative Permeabilities, *Producers Monthly,* 38-41, November 1954.

Dagan, G., Time-Dependent Macrodispersion for Solute Transport in Anisotropic Heterogeneous Aquifers, *Water Resources Research, 24,* (9) 1491-1500, 1988.

deMarsily, G., *Quantitative Hydrogeology,* Academic Press, Orlando, Fl., 1986.

Espedal, M. S., Langlo, P., Saevareid, O., Gislefoss, E., and Hansen, R., Heterogeneous Reservoir Models: Local Refinement and Effective Parameters, Paper SPE-21231, presented at Society of Petroleum Engineers Eleventh Symposium on Reservoir Simulation, Anaheim, CA, February 1991.

Falta, R. W., Javandel, I., Pruess, K. and Witherspoon, P. A., Density-Driven Flow of Gas in the Unsaturated Zone due to the Evaporation of Volatile Organic Compounds, *Water Resources Research, 25,* (10), 2159-2169, 1989.

Falta, R. W., Pruess, K., Javandel, I. and Witherspoon, P. A., Numerical Modeling of Steam Injection for the Removal of Nonaqueous Phase Liquids from the Subsurface. 1. Numerical Formulation, *Water Resources Research, 28,* (2), 433-449, 1992a.

Falta, R. W., Pruess, K., Javandel, I. and Witherspoon, P. A., Numerical Modeling of Steam Injection for the Removal of Nonaqueous Phase Liquids from the Subsurface. 2. Code Validation and Application, *Water Resources Research, 28,* (2), 451-465, 1992b.

Forsythe, G. E., and Wasow, W. R., *Finite-Difference Methods for Partial Differential Equations,* John Wiley and Sons, Inc., New York, London, 1960.

Gelhar, L. W., Welty, C., and Rehfeldt, K. R., A Critical Review of Data on Field-Scale Dispersion in Aquifers, *Water Resources Research, 28,* (7) 1955-1974, 1992.

Glass, R. J., Oosting, G. H., and Steenhuis, T. S., Preferential Solute Transport in Layered Homogeneous Sands as a Consequence of Wetting Front Instability, *Journal Hydrology, 110,* 87-105, 1989.

Glass, R. J., Parlange, J. Y., and Steenhuis, T. S., Immiscible Displacement in Porous Media: Stability Analysis of Three-Dimensional, Axisymmetric Disturbances with Application to Gravity-Driven Wetting Front Instability, *Water Resources Research, 27,* (8) 1947-1956, 1991.

Kueper, B. H. and Frind, E. O., Two-Phase Flow in Heterogeneous Porous Media; 2. Model Application, *Water Resources Research, 27* (6) 1059-1070, 1991.

Kung, K. J. S., Preferential Flow in a Sandy Vadose Zone: 1. Field Observation, *Geoderma, 46,* 51-58, 1990.

Nir, A. and Kirk, B. L., Tracer Theory with Applications in the Geosciences, Report ORNL-5695/PI, Oak Ridge National Laboratory, Oak Ridge, TN, 1982.

Polmann, D. J., McLaughlin, D., Luis, S., Gelhar, L. W., and Ababou, R., Stochastic Modeling of Large-Scale Flow in Heterogeneous Unsaturated Soils, *Water Resources Research, 27,* (7) 1447-1458, 1991.

Poulson, M. M., and Kueper, B. H., A Field Experiment to Study the Behavior of Tetrachloroethylene in Unsaturated Porous Media, *Environmental Science Technology, 26,* (5) 889-895, 1992.

Pruess, K., TOUGH User's Guide, Nuclear Regulatory Commission, Report NUREG/CR-4645, June 1987 (also Lawrence Berkeley Laboratory Report LBL-20700, Berkeley, CA., June 1987).

Pruess, K., TOUGH2 - A General-Purpose Numerical Simulator for Multiphase Fluid and Heat Flow, Lawrence Berkeley Laboratory Report LBL-29400, May 1991a.

Pruess, K., Grid Orientation and Capillary Pressure Effects in the Simulation of Water Injection into Depleted Vapor Zones, *Geothermics, 20,* (5/6), 257-277, 1991b.

Pruess, K. and Bodvarsson, G. S., A Seven-Point Finite Difference Method for Improved Grid Orientation Performance in Pattern Steam Floods, paper SPE-12252, presented at the Seventh Society of Petroleum Engineers Symposium on Reservoir Simulation, San Francisco, 1983.

Pruess, K., and Enedy, S., Numerical Modeling of Injection Experiments at The Geysers, Lawrence Berkeley Laboratory Report LBL-33423, presented at Eighteenth Workshop on Geothermal Resrevoir Engineering, Stanford University, January 26-28, 1993.

Pruess, K. and O'Sullivan, M., Effects of Capillarity and Vapor Adsorption in the Depletion of Vapor-Dominated Geothermal Reservoirs, Lawrence Berkeley Laboratory Report, LBL-31692, presented at Seventeenth Workshop on Geothermal Reservoir Engineering, Stanford University, Stanford, CA, January 1992.

Pullan, A. J., The Quasilinear Approximation for Porous Media Flow, *Water Resources Research, 26,* (6) 1219-1234, 1990.

Sahimi, M., Heiba, A. A., Davis, H. T., and Scriven, L. E., Dispersion in Flow through Porous Media - II: Two-Phase Flow, *Chemical Engineering Science 41,* (8) 2123-2136, 1986.

Scheidegger, A. E., Statistical Hydrodynamics in Porous Media, *Journal Applied Physics, 25,* (8) 994-1001, 1954.

Scheidegger, A. E., *The Physics of Flow through Porous Media,* University of Toronto Press, Toronto and Buffalo, Third Edition, 1974.

Sudicky, E. A., and Huyakorn, P. S., Contaminant Migration in Imperfectly Known Heterogeneous Groundwater Systems, in M. A. Shea (ed.) Contributions in Hydrology, U. S. National Report 1987-1990, American Geophysical Union, pp. 240-253, Washington, D. C., 1991.

Thompson, M. E., Numerical Simulation of Solute Transport in Rough Fractures, *Journal Geophysical Research, 96,* (B3) 4157-4166, 1991.

van Genuchten, T. Th., A Closed-Form Equation for Predicting the Hydraulic Conductivity of Unsaturated Soils, *Soil Science Society America Journal, 44,* 892-898, 1980.

Wheatcraft, S. W., and Cushman, J. H., Hierarchical Approaches to Transport in Porous Media, in: M. A. Shea (editor), Contributions in Hydrology, U. S. National Report 1987-1990, American Geophysical Union, pp. 263-269, Washington, D. C. 1991.

Yanosik, J. L., and McCracken, T. A., A Nine-Point, Finite Difference Reservoir Simulator for Realistic Prediction of Adverse Mobility Ratio Displacements, *Society Petroleum Engineering Journal,* 253-262, August 1979.

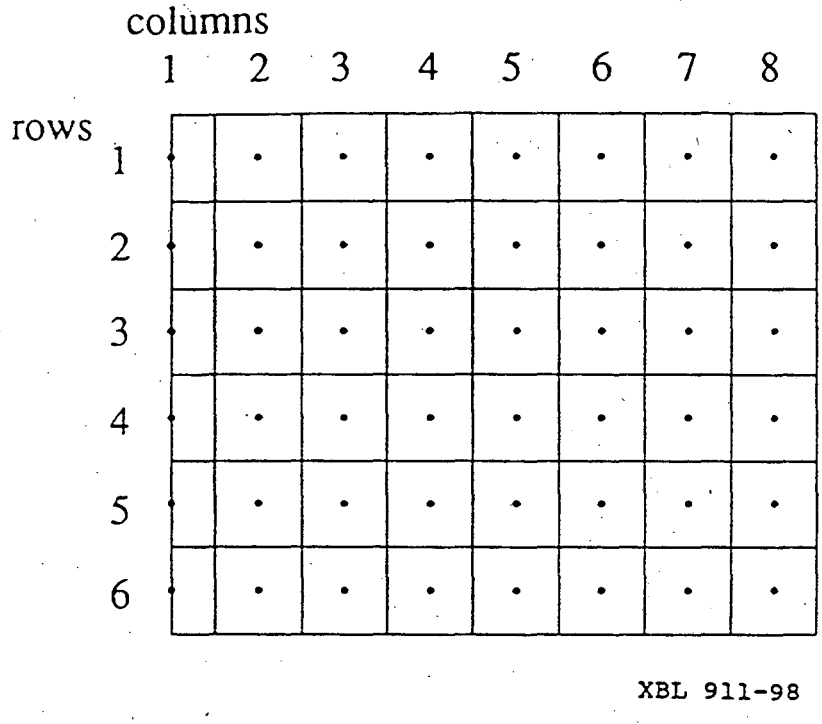

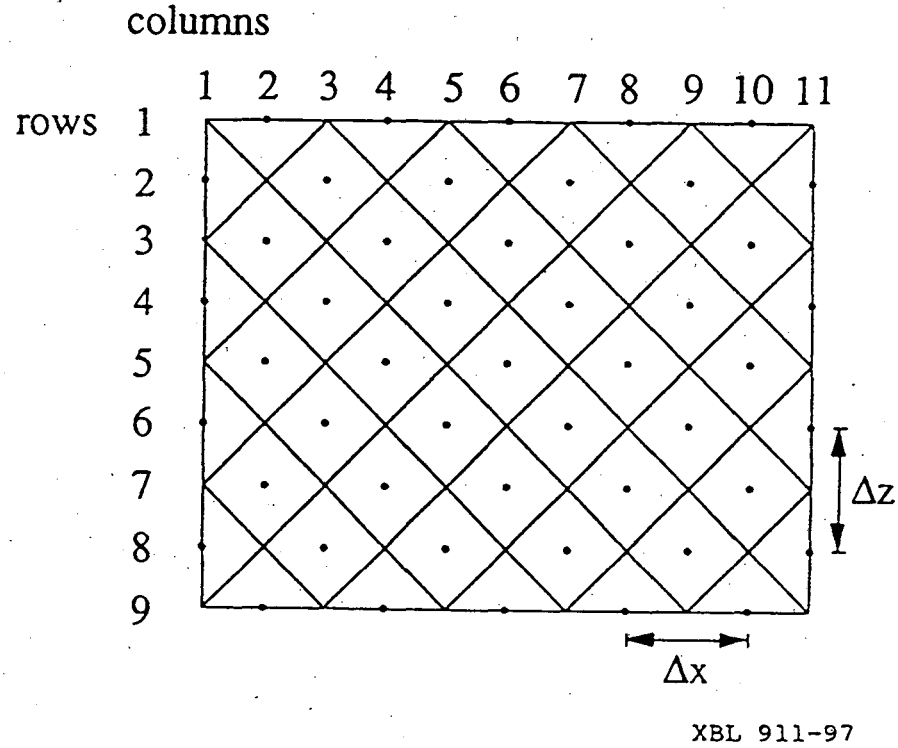

Figure 1. Schematic of parallel and diagonal grids for vertical section models.

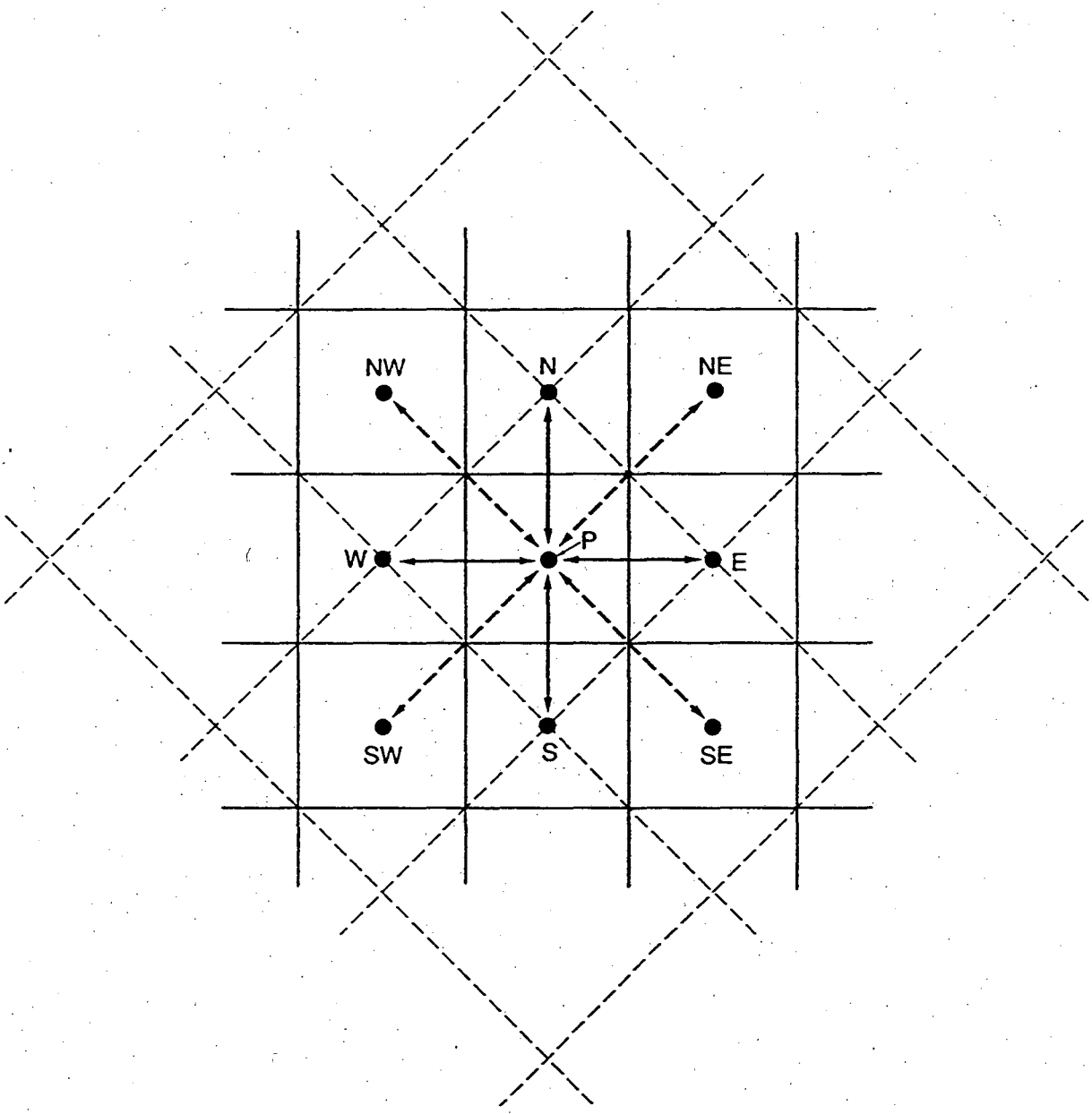

Figure 2. Five- and nine-point finite difference approximations (modified from Pruess and Bodvarsson, 1983).

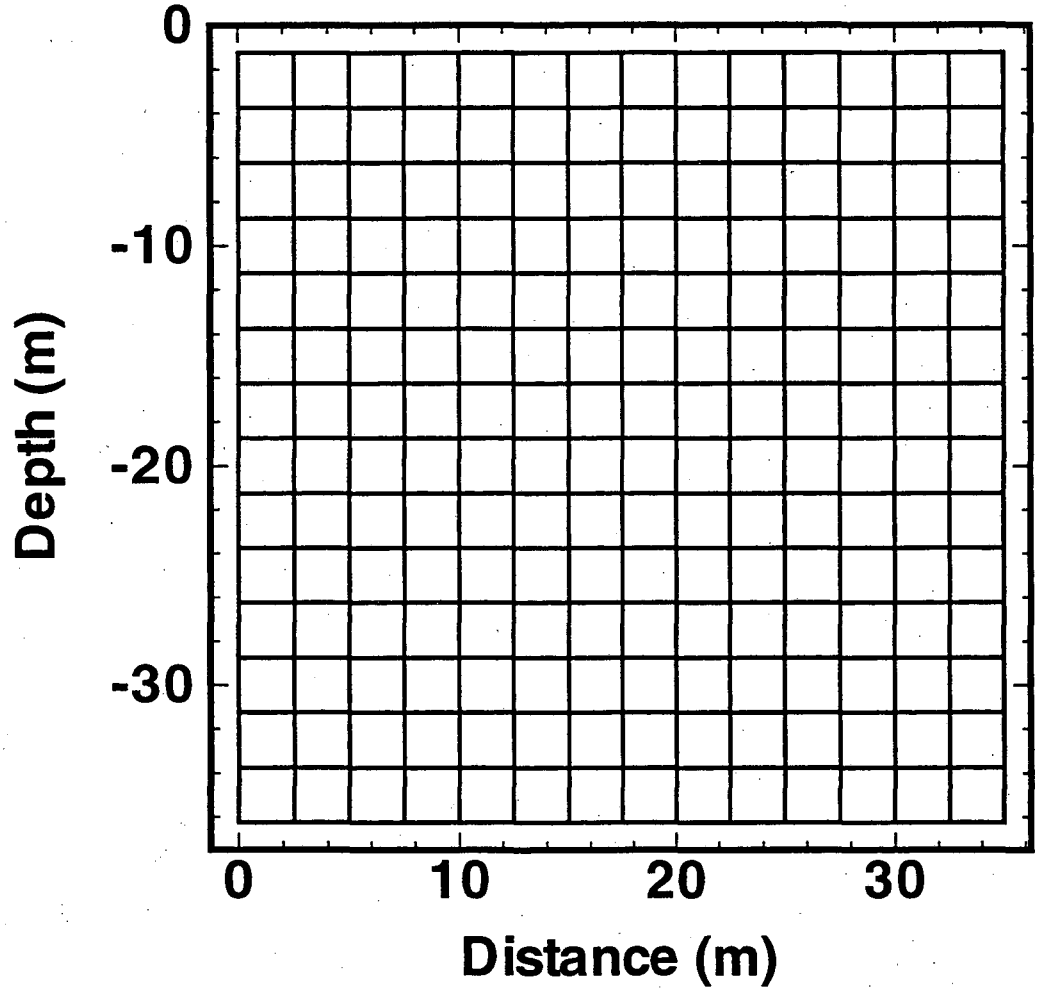

Figure 3. Vertical section grid used for simulating water infiltration into the vadose zone.

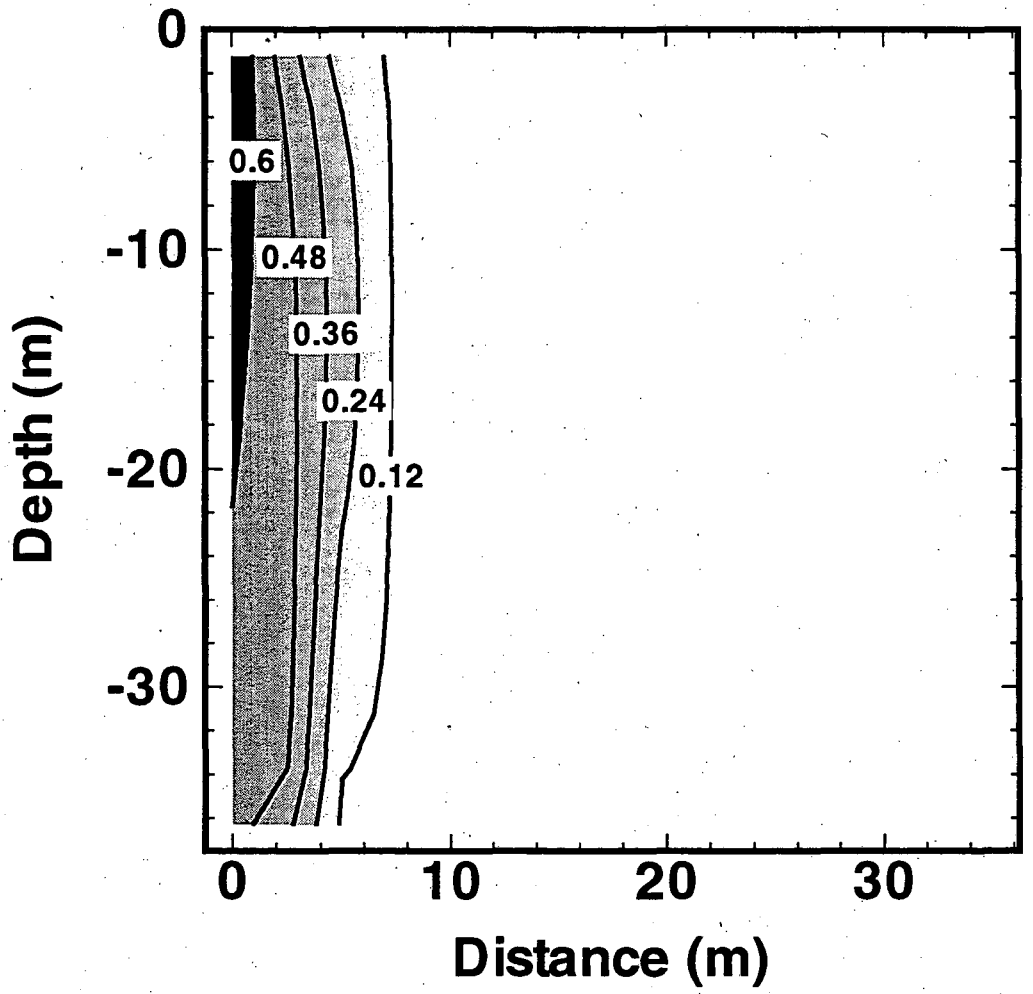

Figure 4. Simulated water infiltration plume after 5.35×10^5 seconds, with a transversal phase dispersivity of $\alpha_T = 0.2$ m. Contour lines of water saturation are shown.

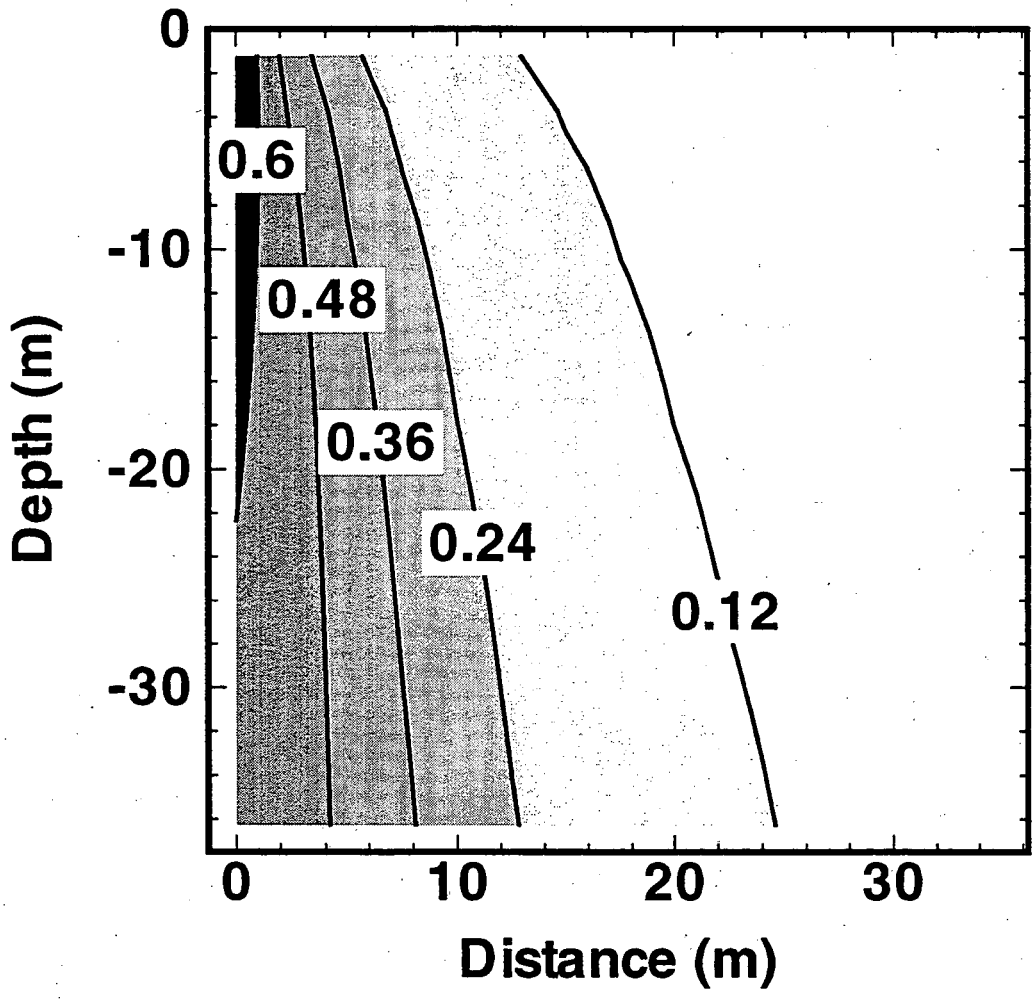

Figure 5. Steady-state water infiltration plume with transversal phase dispersivity of $\alpha_T = 0.2$ m.

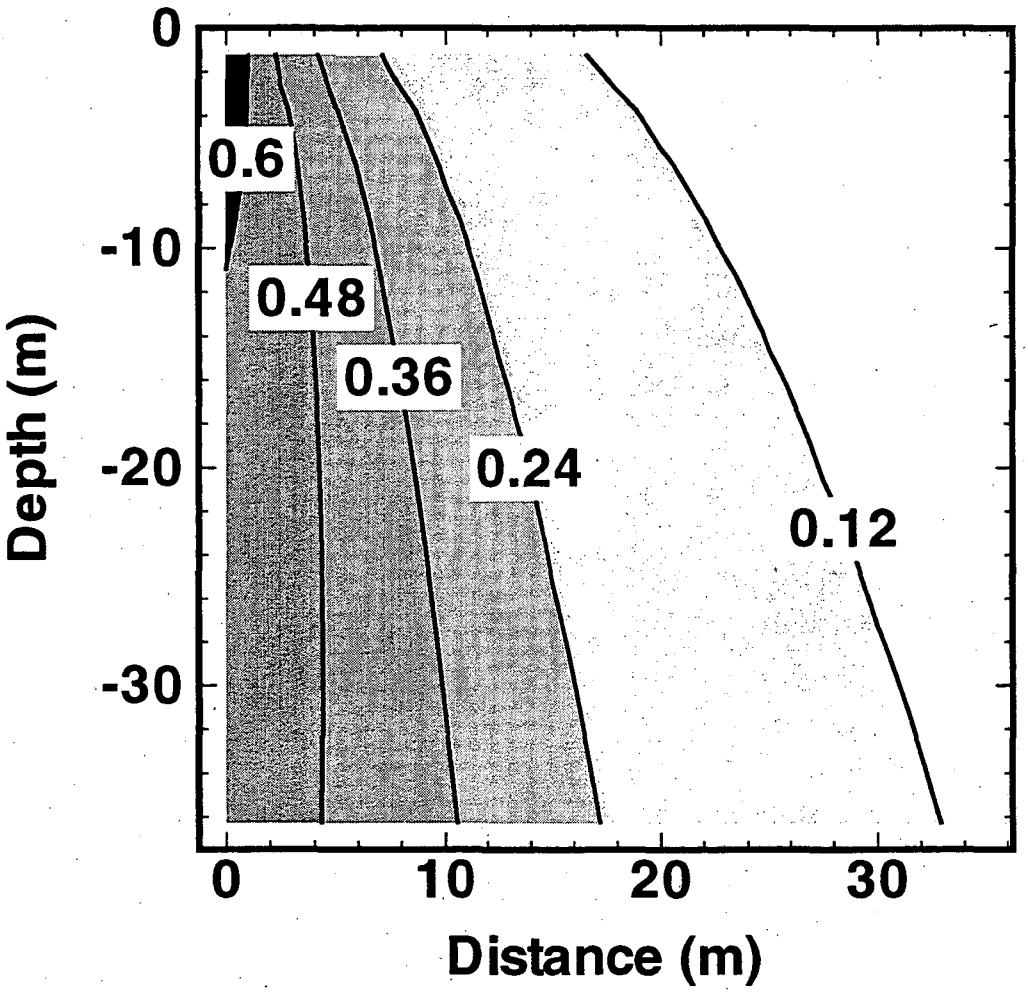

Figure 6. Steady-state water infiltration plume with transversal phase dispersivity of $\alpha_T = 0.4167$ m.

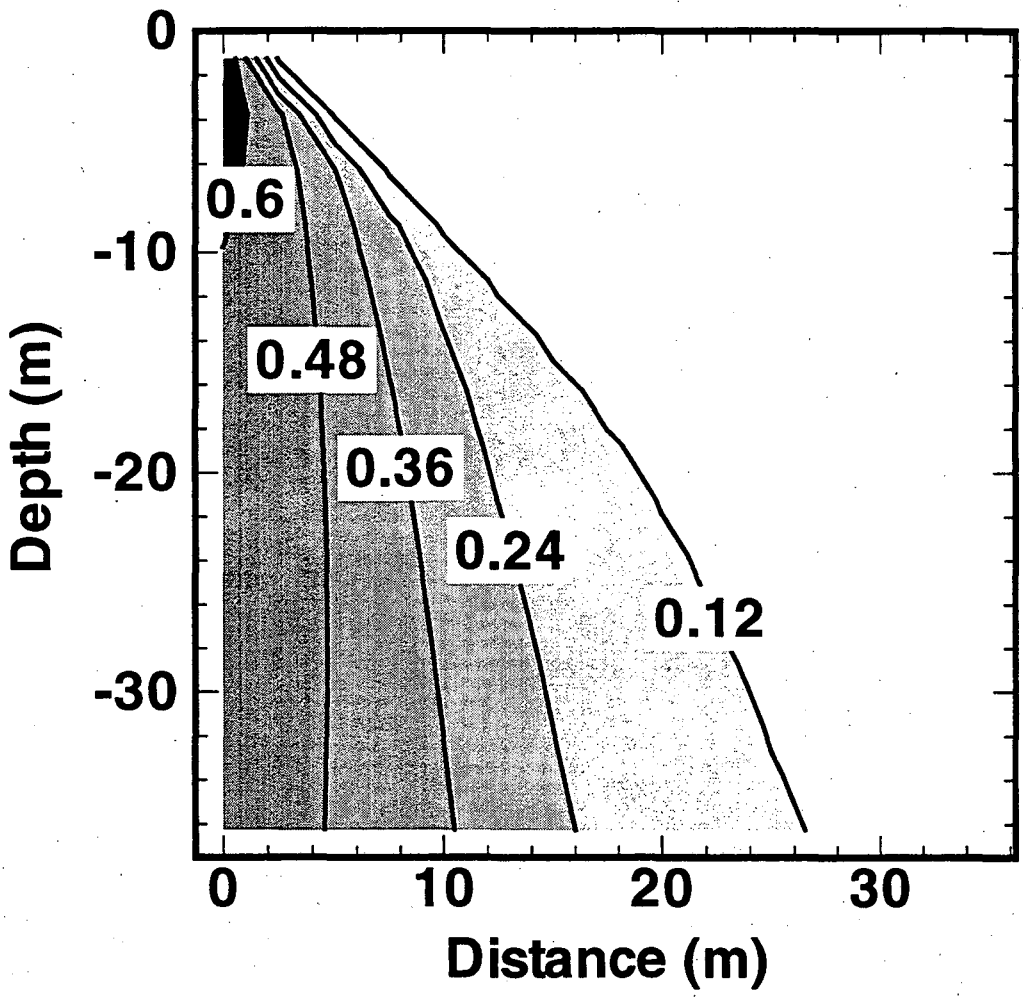

Figure 7. Steady-state water infiltration plume simulated with 9-point parallel grid; no phase dispersion.

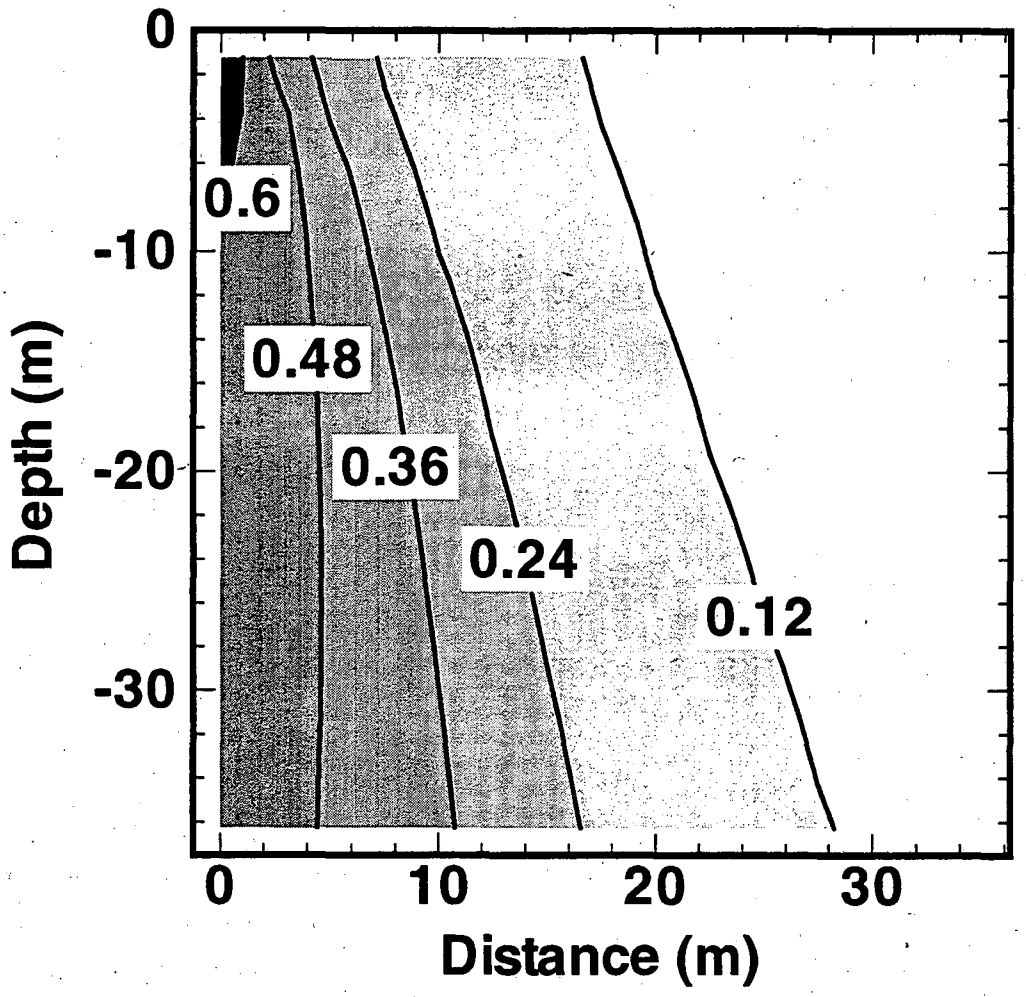

Figure 8. Steady-state water infiltration plume in 9-point parallel grid, no phase dispersion, with upper boundary condition taken from the simulation shown in Fig. 6.

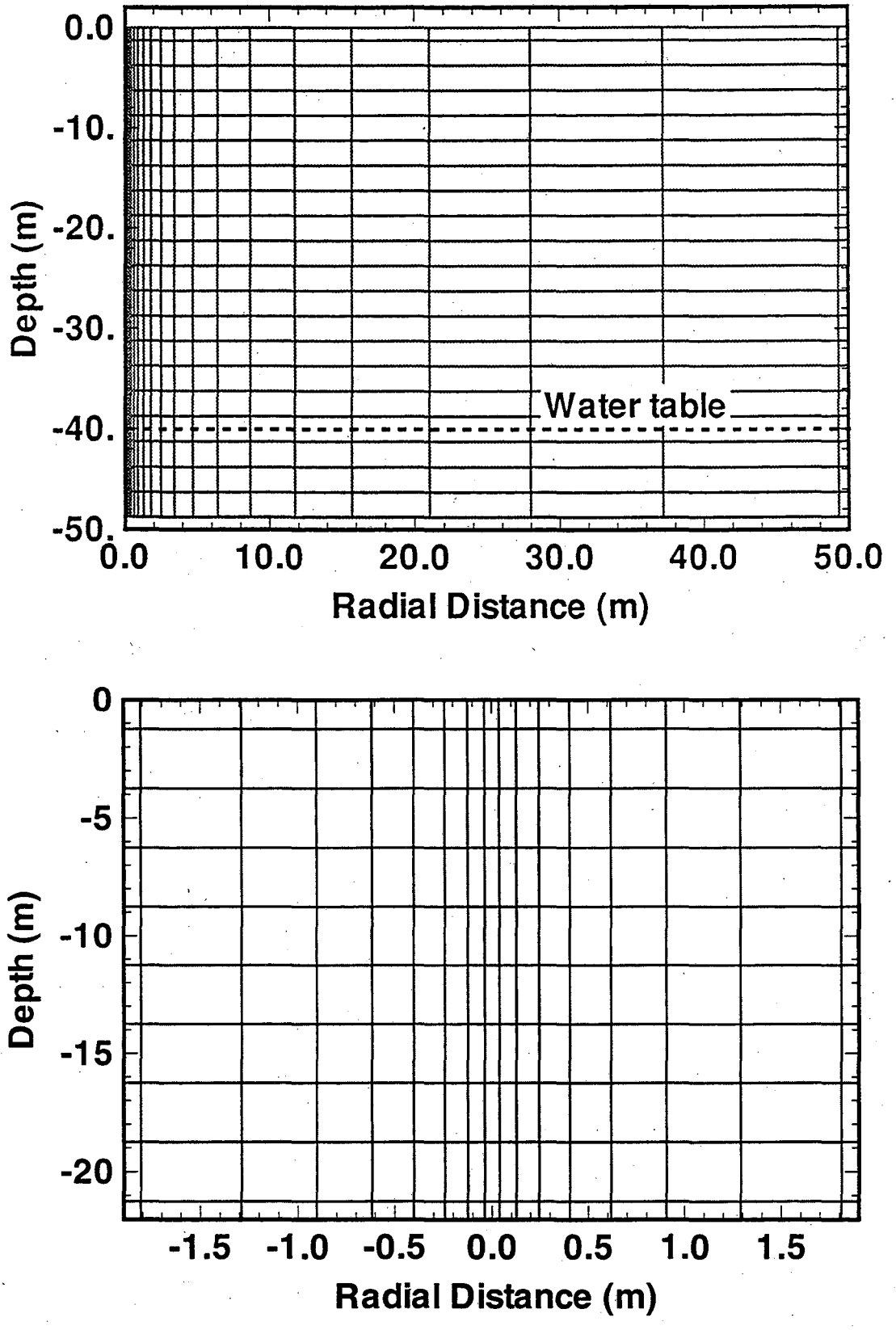

Figure 9. Radially symmetric (R-Z) grid used for simulating a point-like TCE spill. Two expanded views of the grid show the lines connecting nodal points. Grid extends to R = 300 m.

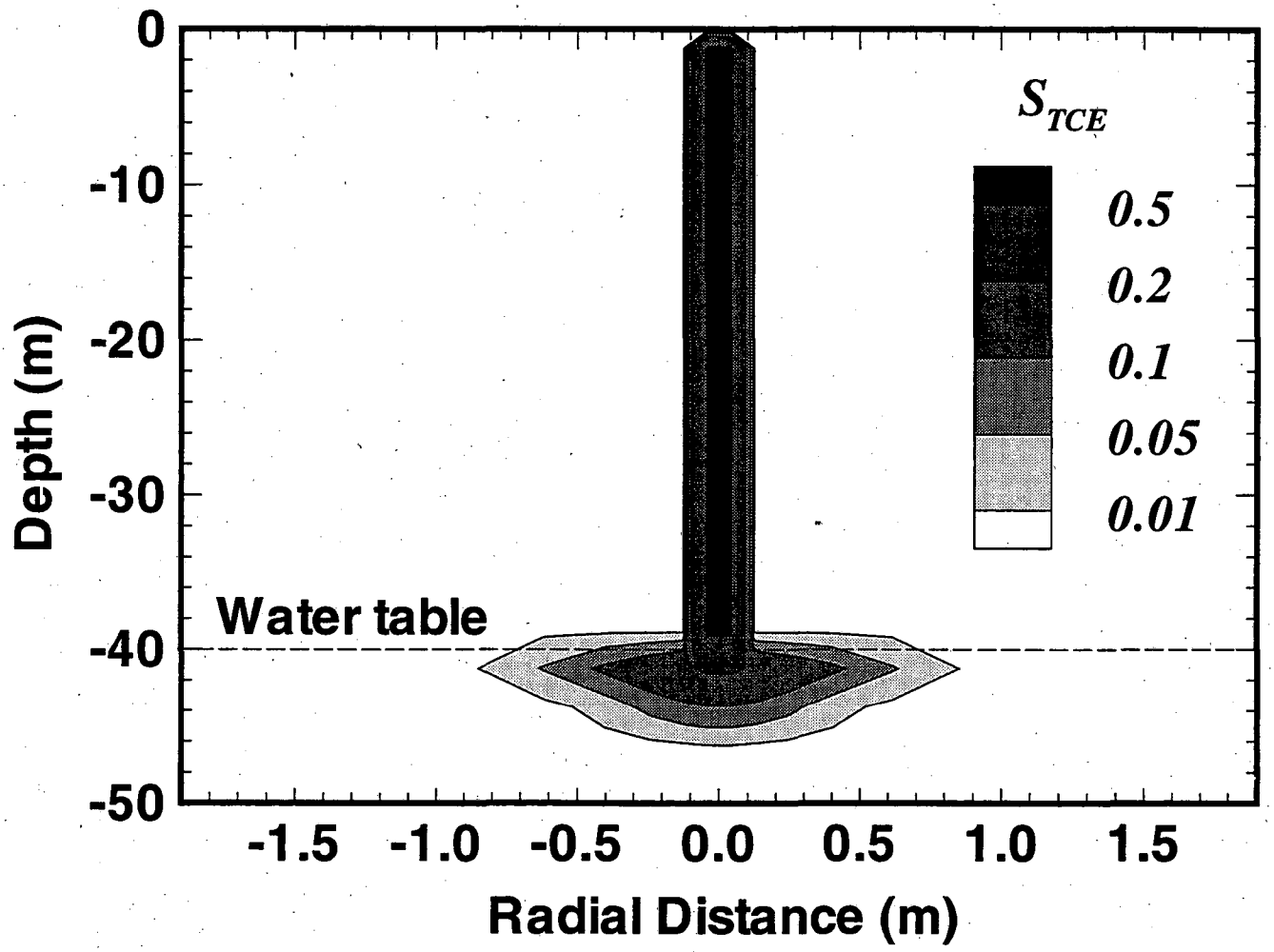

Figure 10. TCE plume simulated with 5-point parallel grid, no phase dispersion, at the end of the 7-day spill period.

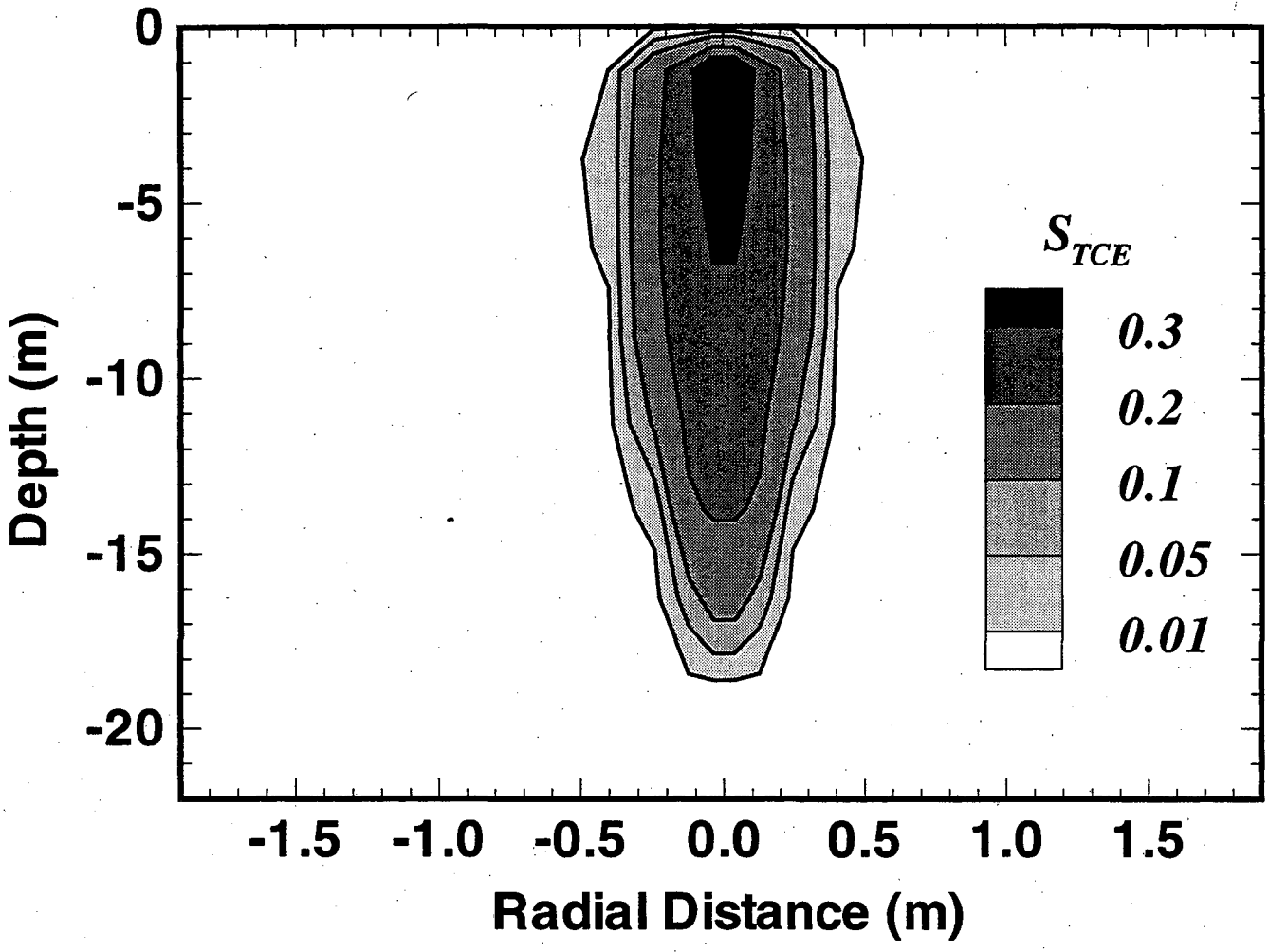

Figure 11. Same as Fig. 10, but phase dispersivity $\alpha_T = 0.002$ m.

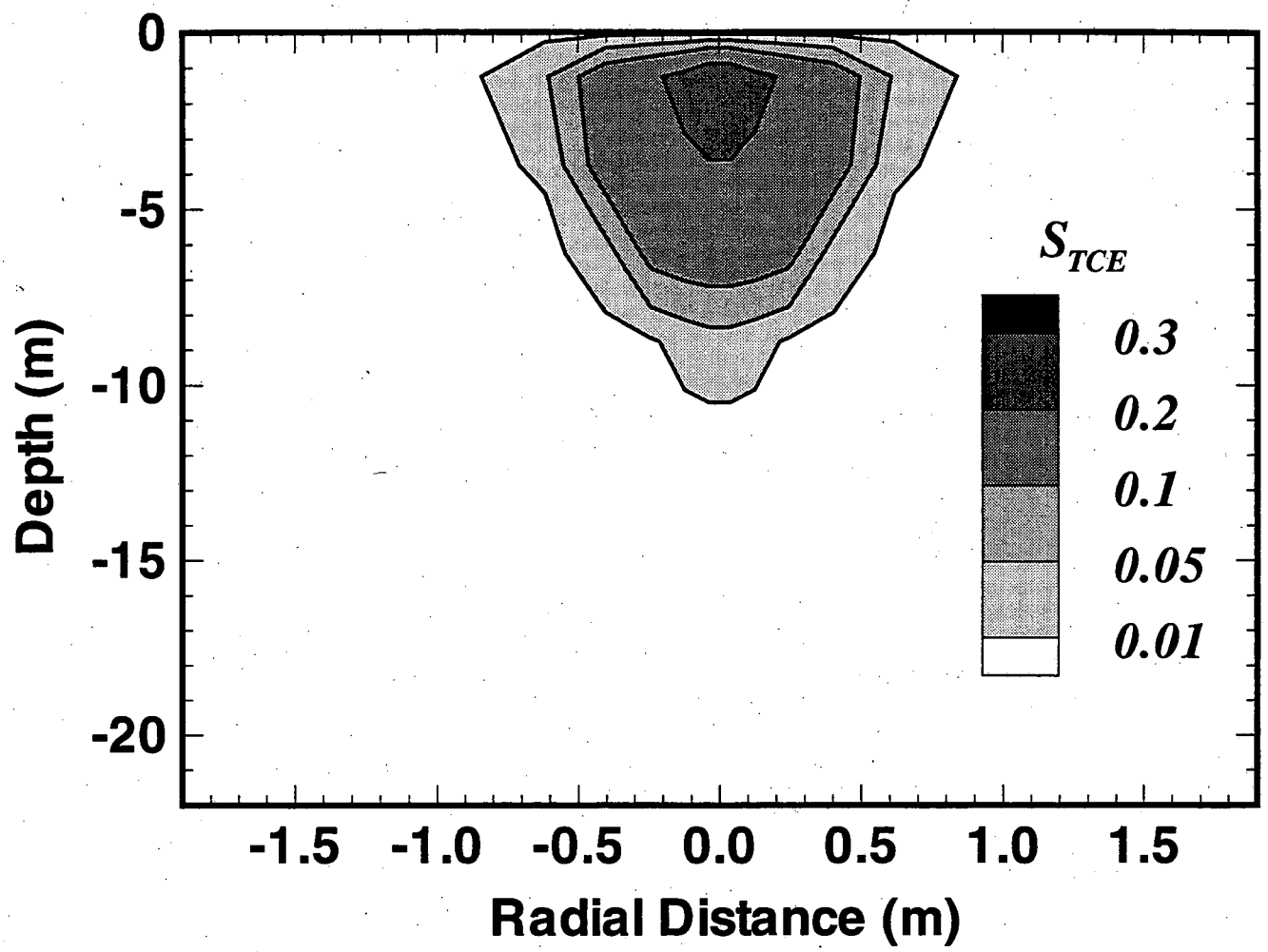

Figure 12. Same as Fig. 10, but phase dispersivity $\alpha_T = 0.02$ m.

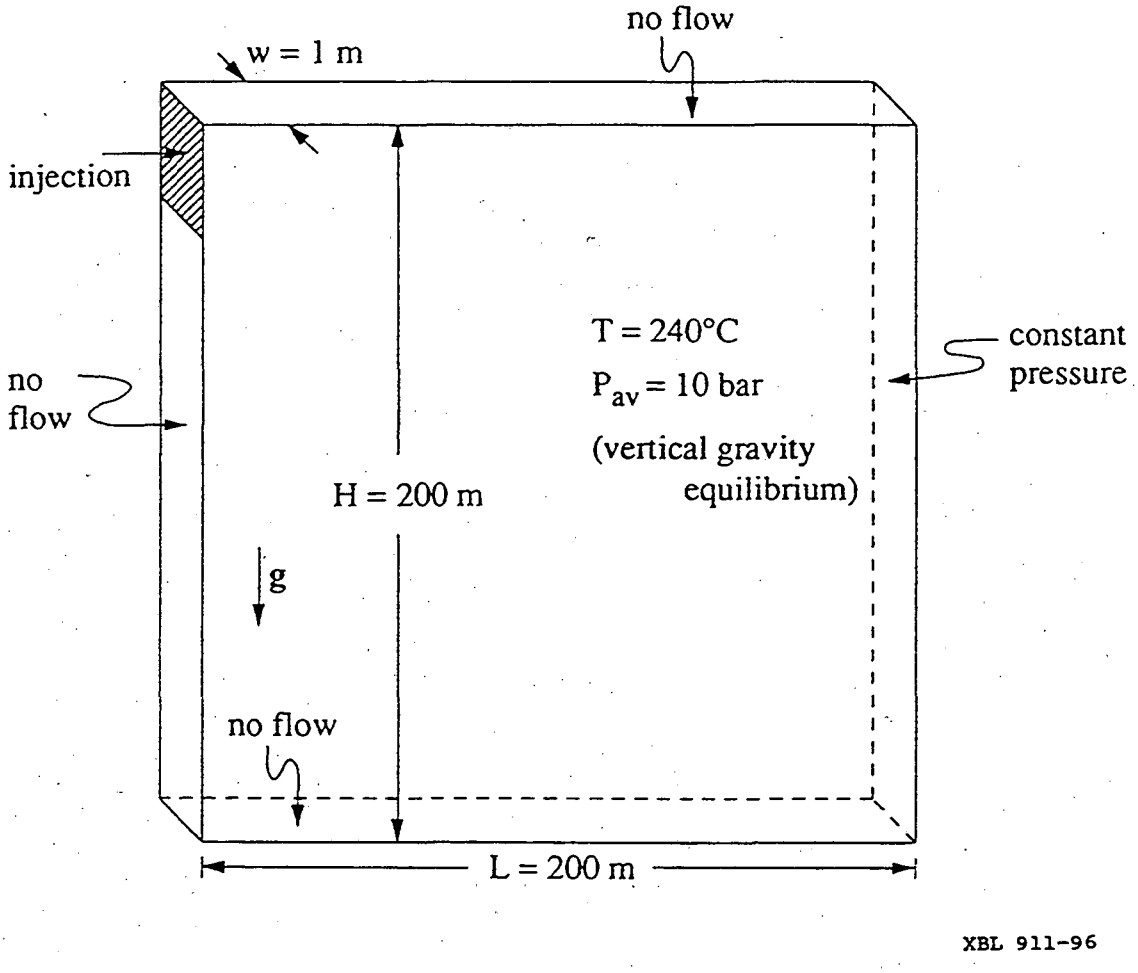

Figure 13. Schematic of 2-D vertical section model for fracture zone in a depleted vapor-dominated geothermal reservoir (from Pruess, 1991b).

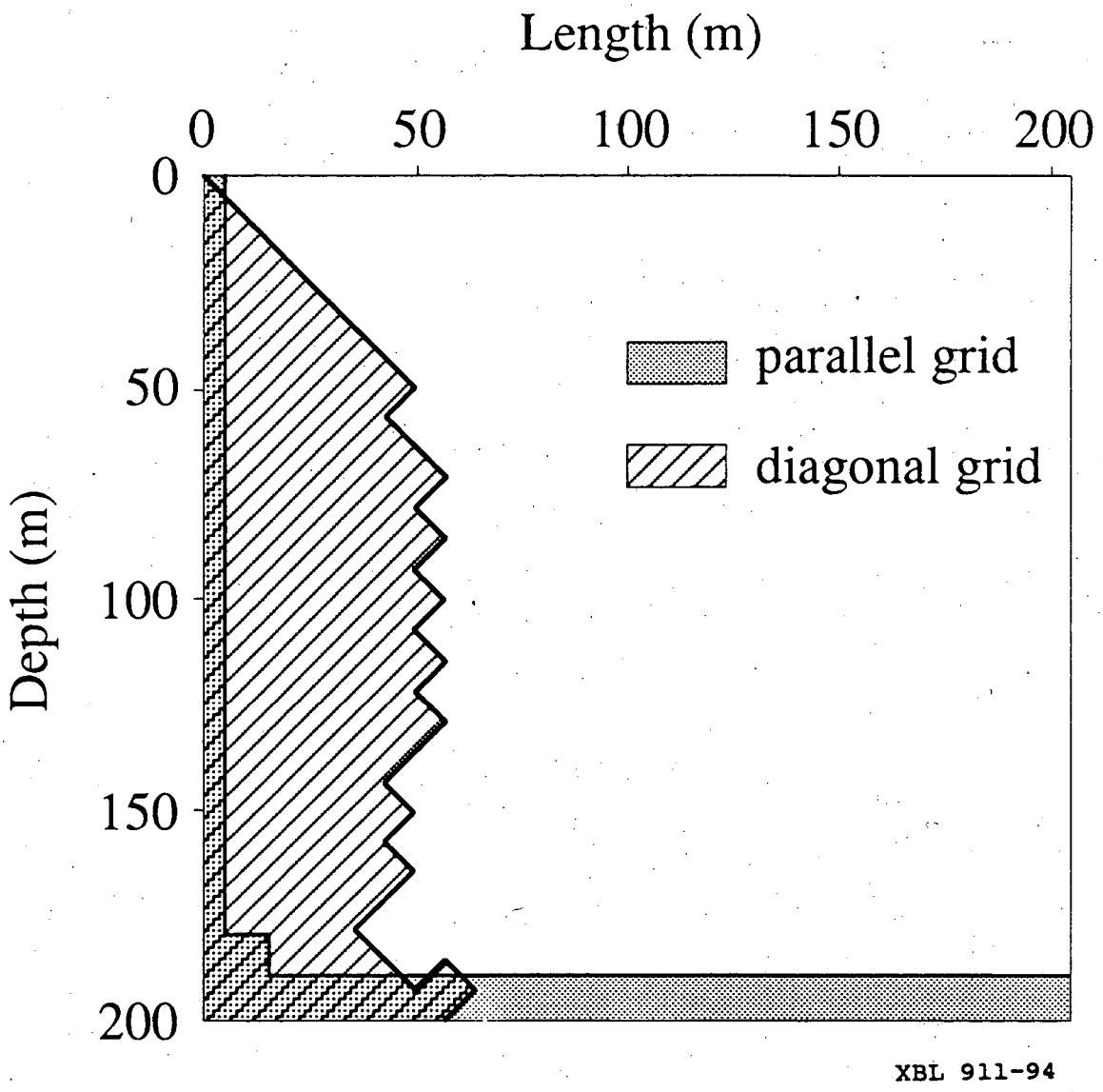

Figure 14. Simulated plumes after 717.01 days of injection in parallel and diagonal 5-point grids (from Pruess, 1991b). Two-phase regions are shaded.

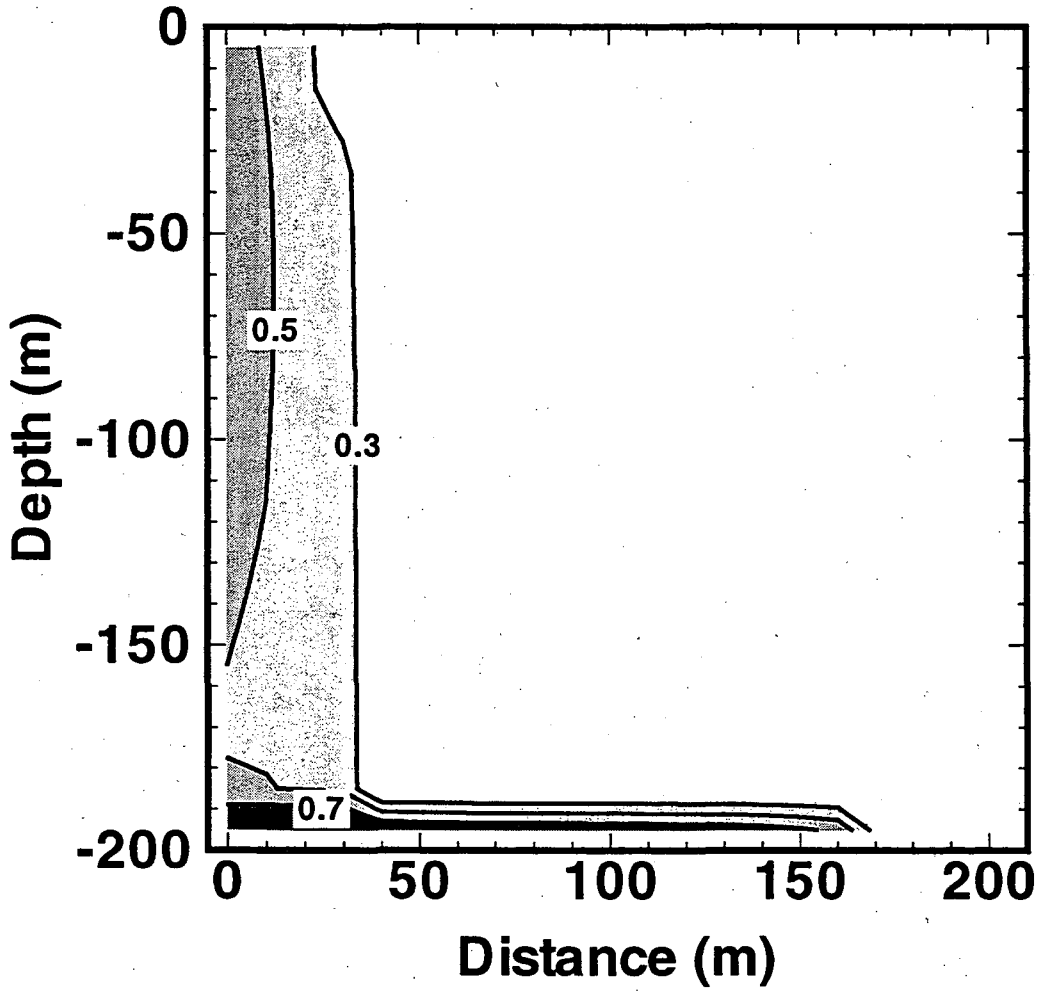

Figure 15. Injection plume after 717.01 days in parallel 5-point grid, with phase dispersivity α_T = 1.67 m. The contour lines show water saturation.

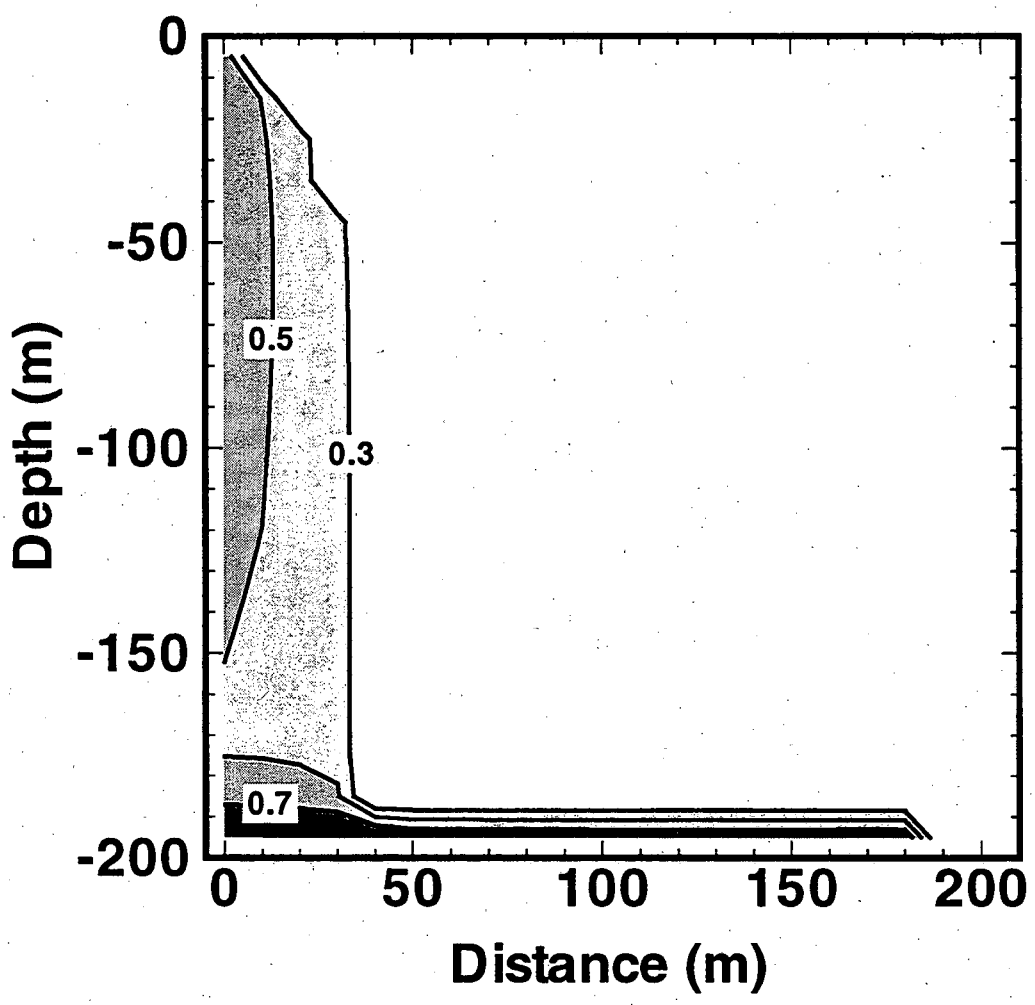

Figure 16. Injection plume after 717.01 days in parallel 9-point grid, no phase dispersion.

LAWRENCE BERKELEY LABORATORY
UNIVERSITY OF CALIFORNIA
TECHNICAL INFORMATION DEPARTMENT
BERKELEY, CALIFORNIA 94720